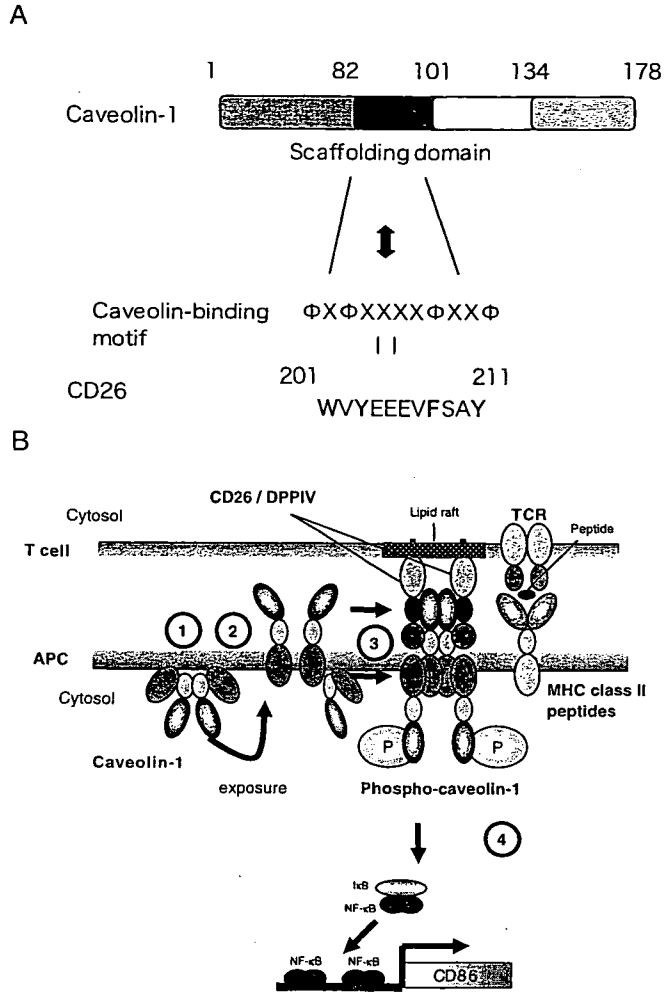

Fig. 3. **A** Schematic representation of human caveolin-1. Residues 1–81 comprise the N-terminal region (NT; *striped rectangle*), residues 82–101 comprise the scaffolding domain (SCD; *black rectangle*), residues 102–134 comprise the transmembrane region (memb; *open rectangle*), and residues 135–178 comprise the C-terminal region (*dotted rectangle*). CD26 contains a caveolin-binding motif (*ΦXΦXXXXΦXXΦ*; *Φ* and *X* depict aromatic residue and any amino acid, respectively), specifically WVYEEEVFSAY in CD26. **B** Model for CD26–caveolin-1 interaction leading to upregulation of CD86. *(1)* Caveolin-1 in monocytes (antigen-presenting cells; *APC*) resides at the inner membrane. *(2)* After uptake of tetanus toxoid into monocytes via caveolae, part of the population of caveolin-1 is exposed on the outer cell surface of tetanus toxoid (TT)-loaded monocytes. *(3)* Migration of CD26+ antigen-specific memory T cells to areas of antigen-loaded APCs results in contact with TT antigen-presenting APC, leading to the association of CD26 and caveolin-1. Aggregation of caveolin-1 in the contact area occurs, presumably by homo-oligomerization (via its residues 61–101), followed by its phosphorylation. *(4)* Phosphorylated caveolin-1 (*phospho-caveolin-1*) transduces signaling leading to activation of NF-κB, resulting in CD86 upregulation. *DPPIV*, dipeptidyl peptidase IV; *TCR*, T-cell receptor; *MHC*, major histocompatibility complex

are named the "caveolin signature motif."[67] Caveolin-1 is composed of 178 amino acid residues (Fig. 3A), and predominantly localized at the plasma membrane, demonstrating a punctuate staining patterns, and in Golgi-derived vesicles.[60] Two isoforms of caveolin-1 (caveolin-1α and β) have been identified, with the β-isoform composed of 31 residue truncated N-terminus of caveolin-1α isoform.[68] Caveolin-1 is composed of the N-terminal hydrophilic domain (residues 1–101), the oligomerization domain (residues 61–101), the scaffolding domain (SCD) (residues 82–101), the membrane spanning domain (residues 102–134), and the C-terminal lipid raft-anchoring domain (residues 135–178).[63] As in trans-Golgi transport, caveolin-1 plays an important role in signal transduction via its SCD, which compartmentalizes a multitude of signaling molecules.[63,69] These include G proteins, epidermal growth factor receptor, insulin receptor, endothelial nitric oxide synthase (eNOS), nonreceptor tyrosine kinase (Src, Fyn, Yes), flotillins, Ser/Thr kinases (PKA, Raf, MAPK, PI3K, Grb2), and catenins.[63,69] Other cellular functions of caveolin-1 are related to the lipid metabolism, especially to cholesterol scavenging in macrophages.[70] However, it is unknown whether caveolin-1 also plays a role in signal transduction in APCs. Although CD26 was present in caveolae of fibroblast-like synoviocytes,[71] direct CD26–cavolin-1 interaction and associated signaling events have not been demonstrated in immune cells. Interestingly, caveolin-1 knockout mice show defects in the angiogenic response to exogenous stimuli, such as Matrigel plugs containing angiogenic growth factors (bFGF) or tumors.[72] In this context, angiogenic vessels density and penetration was significantly reduced in caveolin-1 null mice. Moreover, electron microscopic examination revealed incomplete de novo capillary formation in tumors implanted within caveolin-1 null mice. Thus, it appears that caveolin-1 null mice have a defect in endothelial cell differentiation. This is consistent with in vitro observations demonstrating that overexpression of caveolin-1 enhances endothelial capillary-tube formation, while downregulation of caveolin-1 using an anti-sense approach blocks endothelial tube formation.[73] With regards to inflammation and caveolin-1, a series of elegant experiments showed that caveolin-1 has a role in inflammation with association of eNOS.[74] Using a cell permeable peptides link to the caveolin-1 scaffolding domain in aortic explants, the potent eNOS inhibiting activity of caveolin-1 was demonstrated. In vivo delivery of this peptide resulted in significant decreases in acute inflammation and edema resulting from vascular permeability. Taken together, these findings demonstrate an important relationship between caveolin-1 and vascularization, with implication for capillary formation in inflammatory processes.

Caveolin-1: CD26 binding protein in APC

Since CD26 on human T cells was identified as an activation antigen and costimulatory molecule of the TCR complex, several binding proteins to CD26 have been described. As described above, multiple chemokines interact with CD26/DPPIV as its substrates, and other proteins such as ADA, fibronectin, thromboxane A2 receptor, and CXCR4 are shown to be associated with CD26.[49,75–78] However, the precise mechanism involved in T-cell activation in response to memory antigen such as TT remains to be clearly characterized. Recently, we demonstrated that CD26 binds to

caveolin-1 on APC, and that residues 201–211 of CD26 along with the serine catalytic site at residue 630, which constitute a pocket structure of CD26/DPPIV, contribute to binding to the caveolin-1 scaffolding domain (Fig. 3A).[31] This region in CD26 contains a caveolin-binding domain (CBD) ($\Phi X\Phi XXXX\Phi XX\Phi$; Φ and X depict aromatic residue and any amino acid, respectively), specifically WVYEEEVFSAY in CD26.[48,69] These observations strongly support the notion that DPPIV enzyme activity is necessary to exert TCR-costimulatory activation via CD26.[48] In addition, following CD26–cavolin-1 interaction on TT-loaded monocytes, caveolin-1 is phosphorylated, with linkage to NF-κB activation, followed by upregulation of CD86. Finally, reduced caveolin-1 expression on monocytes inhibits CD26-mediated CD86 upregulation and abrogates CD26 effect on TT-induced T-cell proliferation (Fig. 3B). Taken together, these results strongly suggest that CD26–cavolin-1 interaction plays a role in the upregulation of CD86 on TT-loaded monocytes and subsequent engagement with CD28 on T cells, leading to antigen-specific T-cell activation.

Caveolin-1 has been reported to be an integral membrane protein with a cytoplasmic N-terminal domain and a cytoplasmic C-terminal domain.[63] Our data showed that the N-terminal domain of caveolin-1 was expressed on the cell surface of monocytes 12–24h after tetanus toxoid was loaded (Fig. 4A). Since tetanus toxoid was trafficked in cells through caveolae,[79,80] caveolin-1 may be transported along with the peptide-MHC complex in APC, and is then expressed on cell surface by the antigen-processing machinery for T-cell contact.[80–82] The data shown in Fig. 4B indicated that CD26 on activated memory T cells directly faces caveolin-1 on TT-loaded monocytes in the contact area, which is the immunological synapse for T cell-APC interaction. It is conceivable that the interaction of CD26 with caveolin-1 on antigen-loaded monocytes results in CD86 upregulation, therefore enhancing the subsequent interaction of CD86 and CD28 on T cells to induce antigen-specific T-cell proliferation and activation.

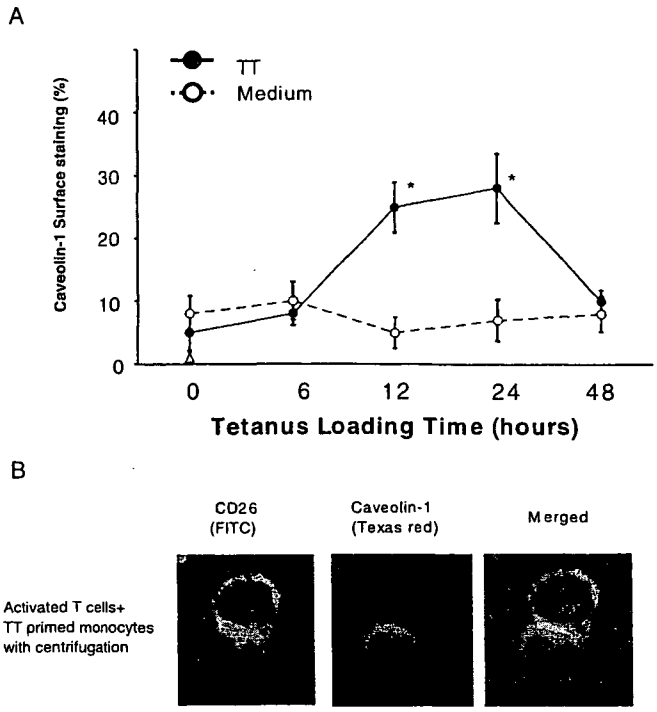

Fig. 4A,B. Immunocytochemical analysis of caveolin-1 and CD26 interaction. **A** Caveolin-1 in monocytes was exposed to cell surface after tetanus toxoid (*TT*) treatment, and interacted with CD26 on activated T cells. After purified monocytes were incubated with (*solid circle*) or without (*open circle*) TT, cell surface caveolin-1 was stained with anti-caveolin-1 antibody detecting the N terminal region, and analyzed for % positive cells by flow cytometry. Data of % positive cells represent mean ± SE from five independent experiments. *Asterisks* indicate points of significant increase. **B** To form cell–cell conjugation, activated T cells and TT-loaded monocytes were mixed, followed by centrifugation. Conjugates were fixed without permeabilization, and stained with anti-CD26 (fluorescein isothiocyanate) and anti-caveolin-1 (Texas red) antibodies. *Bars* 10μm

CD26 and caveolin-1 in synovitis

Rheumatoid arthritis is a classical example of an immune-mediated disease with chronically smoldering injury of the synovial joints resulting from infiltration of inflammatory cells, and synovitis of diarthrodial joints is its most visible manifestation. Although the observed architectures of rheumatoid synovitis vary in different individuals with RA as well as at various disease stages, the most frequent type of rheumatoid synovitis is a diffuse inflammatory infiltrate in which T cells, B cells, and macrophages are scattered around increased vasculature and synoviocytes. Meanwhile, in the remaining 40–50% of patients with RA, infiltrating inflammatory cells organize themselves into follicular structures.[1] It is known that the inflammatory activation events in rheumatoid synovitis are dependent upon cell–cell contact among T cells, fibroblast-like synoviocytes, APCs, and regional tissues such as type II collagen and proteoglycan.[83] Moreover, previous reports showed that CD26+ T cells exhibit strong migratory ability through endothelial cells, and are present at high levels in the rheumatoid synovium and the synovial fluids.[20,22,23] These findings suggest that T cells with high levels of CD26 antigen may preferentially migrate into the rheumatoid synovium to induce inflammation and tissue destruction. To test this hypothesis, we examined the expression of CD26 and caveolin-1 in the rheumatoid synovium through immunohistochemistry. As shown in Fig. 5A, CD26+ lymphoid cells are clearly observed in diffuse synovitis. In follicular synovitis examined with the sequential sections, CD26+ lymphoid cells are infiltrated in the sublining area of caveolin-1-positive synovial cells (arrow in panel b of Fig. 5B), and are adjacent to caveolin-1-positive inflammatory cells (arrowheads in panel c of Fig. 5B). Moreover, the intimal lining layer is hyperplastic with multiple layers, and the synoviocytes in these layers highly express caveolin-1 (arrow in Fig. 5C). In addition, CD86 and caveolin-1 are coexpressed in the intimal lining synoviocytes and the sublining fibroblast-like synovial cells (black arrowhead in Fig. 5C). Furthermore, increased vas-

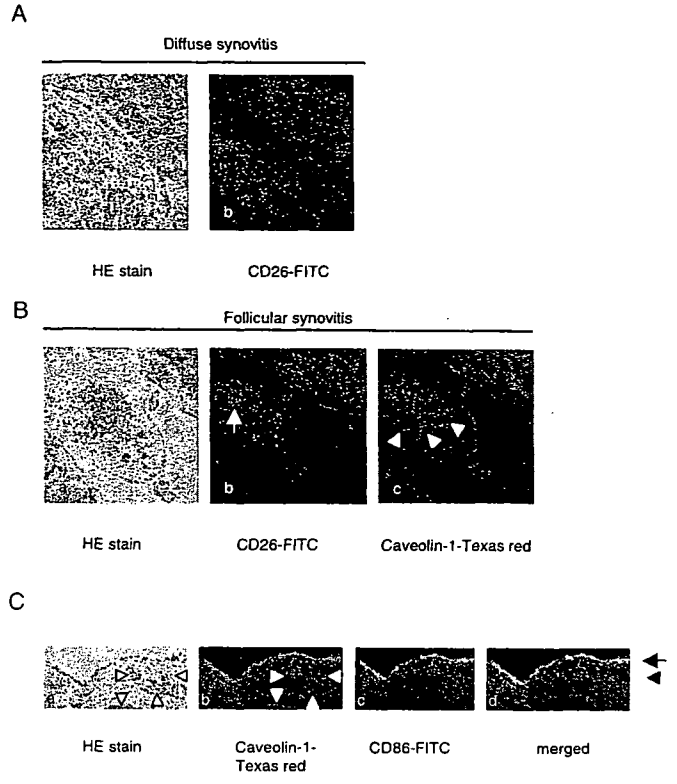

Fig. 5A–C. Architecture and immunohistochemistry of rheumatoid synovitis. **A** *Panel a* shows H&E-stained histology of diffuse synovitis with inflammatory cells intermingled with fibroblast-like synoviocytes (×100). *Panel b* shows immunohistochemistry of the sequential section of panel a, which was stained with fluorescein isothiocyanate (FITC)-conjugated anti-CD26 antibody (×100). **B** *Panel a* shows H&E-stained histology of follicular synovitis with germinal center formation (×100). *Panel b* shows immunohistochemistry of the sequential section of panel a, which was stained with FITC-conjugated anti-CD26 antibody. This reveals that CD26-positive lymphoid cells are scattered around the follicles (*arrow*) (×100). *Panel c* shows immunohistochemistry of the sequential section of panel b, which was stained with anti-caveolin-1 (Texas red). This reveals that the intimal lining synoviocytes and the sublining fibroblast-like synoviocytes adjacent to CD26+ lymphoid cells (arrow head) express caveolin-1 (×100). **C** *Panel a* shows synovial histology of rheumatoid arthritis with H&E staining (×100). *Panels b and c* show immunohistochemistry of the sequential section of panel a which was stained with caveolin-1 (Texas red) and CD86 (FITC), simultaneously. *Panel d* shows the merged view of panels b and c. *Arrow* shows the intimal lining synoviocytes, and *black arrowhead* shows the sublining fibroblast-like synoviocytes. *White arrowheads* show the increased vascularization in synovitis

cularization is seen in synovitis, and caveolin-1 is preferentially expressed in the luminar surface of endothelial cells in the rheumatoid synovium (white arrowheads in Fig. 5C). Taken together, we propose a model to describe the molecular events in monocytes leading to activation that are triggered by CD26–cavolin-1 interaction in rheumatoid synovium (Fig. 6). The initial step of inflammation in the synovium proceeds from activation of CD26+ T cells by APC and/or rheumatoid synoviocytes via presentation of a yet-to-be-identified antigen, concomitant with costimulation via such pairing as CD28–B7 and CD26–cavolin-1 (phase 1 in Fig. 6). With regard to the interaction between T cell–APC and the resultant immune response, entry of antigens via caveolae into APC leads to presentation of antigen peptides on MHC class II molecules and exposure of caveolin-1 (inside box in phase 1 of Fig. 6). APC thus induces the activation of memory T cells through the TCR and costimulatory molecules such as CD86/CD80–CD28, leading to the formation of mature immunological synapses. Following the association between caveolin-1 on APC and CD26 on memory T cells, CD86 is upregulated on APC surface, and memory T cells are subsequently activated via the costimulatory effect of CD26 on TCR activation. By enhancing TCR activation via CD26–cavolin-1 interaction, prolongation of the immunological synapse may be maintained. CD86 upregulation therefore results in potent T cell–APC interaction, leading to the development of activated memory T cells locally and activation of the immune response, as well as the subsequent development of rheumatoid synovitis. After triggering inflammation of the synovium, memory T-cell activation leads to progression of inflammation in rheumatoid synovium, i.e., infiltration of inflammatory cells, increase of vascular vessels, formation of follicular germinal centers, and proliferation of synoviocytes (phase 2 in Fig. 6). Destructive inflammation then progresses to cartilage and bone injury by pannus (phase 3 in Fig. 6). As a result, progressive inflammation leads to synovial membrane invasion of bone, loss of cartilage and bone destruction in joints.

Molecular-targeted therapeutic strategies in RA

Although the specific antigens responsible for the pathogenesis of RA have not been identified, T-cell activation via interaction with APCs plays a pivotal role in disease development. In this regard, therapeutic strategies have targeted cellular pathways in RA. In addition to anti-cytokine reagents, impressive therapeutic effect has been recently reported following the blocking of CD28-mediated costimulation by the use of cytotoxic T-lymphocyte-associated antigen 4-IgG1 (CTLA4Ig).[84,85] Expressed on T cells within hours to days after activation,[86,87] CTLA4 is the high-avidity receptor for both CD80 and CD86, and inhibits T-cell proliferation and IL-2 production.[88,89] A fusion protein, CTLA4Ig binds both CD80 and CD86 on APCs, thereby preventing these molecules from engaging CD28 on T cells.[90] By blocking the engagement of CD28, CTLA4Ig prevents the delivery of the second costimulatory signal that is required for optimal activation of T cells. The successful usage of this agent therefore demonstrates that blocking costimulatory signal to inhibit T-cell activation is a novel and promising therapeutic concept for selected autoimmune diseases.[84,85] In this regard, since we showed that CD26–cavolin-1 interaction may play a pivotal role in rheumatoid synovitis, reagents capable of blocking CD26–cavolin-1 interaction in synovitis may be potentially useful in the treatment of patients with RA.

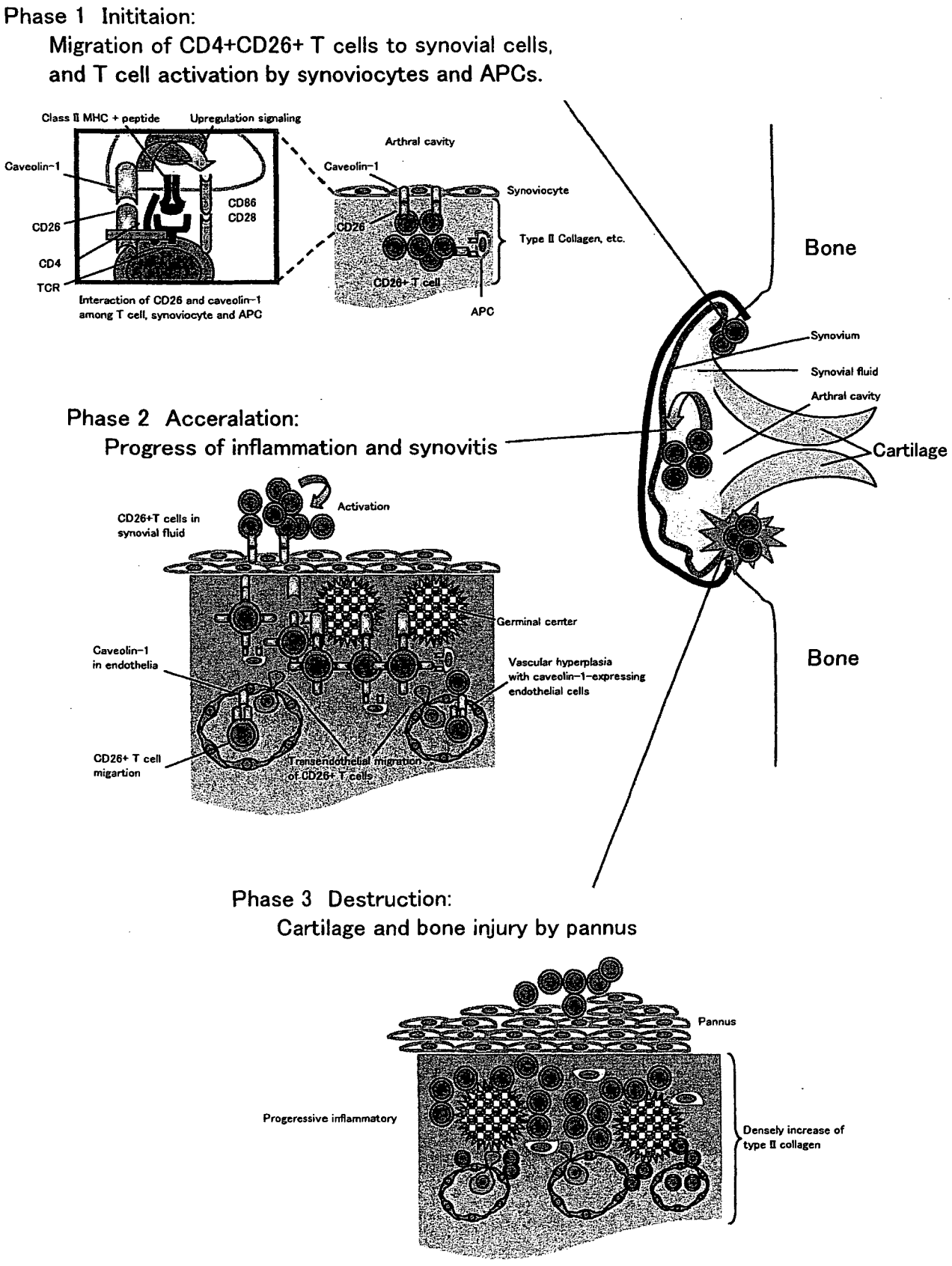

Fig. 6. Schematic diagram of inflammatory progress in rheumatoid synovitis. See text for details

Conclusions

Our results may thus provide a new approach to the treatment of autoimmune diseases or other immune-mediated disorders by directly intervening with the interaction between activated T-cell and APC. Targeting the binding of the pocket structure of CD26 and the scaffolding domain of caveolin-1 may lead to novel therapeutic approaches, including the utilization of antagonists that regulate antigen-specific immune response in immune-mediated disorders such as RA.

Acknowledgments This work was supported by Grants-in-Aid from the Ministry of Education, Science, Sports and Culture (K.O. and C.M.), and Ministry of Health, Labor, and Welfare, Japan (C.M.).

References

1. Goronzy JJ, Weyand CM. Rheumatoid arthritis. Immunol Rev 2005;204:55–73.
2. Mor A, Abramson SB, Pillinger MH. The fibroblast-like synovial cell in rheumatoid arthritis: a key player in inflammation and joint destruction. Clin Immunol 2005;115(2):118–28.
3. Yamada R, Tanaka T, Unoki M, Nagai T, Sawada T, Ohnishi Y, et al. Association between a single-nucleotide polymorphism in the promoter of the human interleukin-3 gene and rheumatoid arthritis in Japanese patients, and maximum-likelihood estimation of combinatorial effect that two genetic loci have on susceptibility to the disease. Am J Hum Genet 2001;68(3):674–85.
4. Elliott MJ, Maini RN, Feldmann M, Kalden JR, Antoni C, Smolen JS, et al. Randomised double-blind comparison of chimeric monoclonal antibody to tumour necrosis factor alpha (cA2) versus placebo in rheumatoid arthritis. Lancet 1994;344(8930):1105–10.
5. Bresnihan B, Alvaro-Gracia JM, Cobby M, Doherty M, Domljan Z, Emery P, et al. Treatment of rheumatoid arthritis with recombinant human interleukin-1 receptor antagonist. Arthritis Rheum 1998;41(12):2196–204.
6. Maini RN, Breedveld FC, Kalden JR, Smolen JS, Davis D, Macfarlane JD, et al. Therapeutic efficacy of multiple intravenous infusions of anti-tumor necrosis factor alpha monoclonal antibody combined with low-dose weekly methotrexate in rheumatoid arthritis. Arthritis Rheum 1998;41(9):1552–63.
7. Moreland LW, Baumgartner SW, Schiff MH, Tindall EA, Fleischmann RM, Weaver AL, et al. Treatment of rheumatoid arthritis with a recombinant human tumor necrosis factor receptor (p75)-Fc fusion protein. N Engl J Med 1997;337(3):141–7.
8. Bathon JM, Martin RW, Fleischmann RM, Tesser JR, Schiff MH, Keystone EC, et al. A comparison of etanercept and methotrexate in patients with early rheumatoid arthritis. N Engl J Med 2000;343(22):1586–93.
9. Lipsky PE, van der Heijde DM, St Clair EW, Furst DE, Breedveld FC, Kalden JR, et al. Infliximab and methotrexate in the treatment of rheumatoid arthritis. Anti-Tumor Necrosis Factor Trial in Rheumatoid Arthritis with Concomitant Therapy Study Group. N Engl J Med 2000;343(22):1594–602.
10. Moreland LW, Schiff MH, Baumgartner SW, Tindall EA, Fleischmann RM, Bulpitt KJ, et al. Etanercept therapy in rheumatoid arthritis. A randomized, controlled trial. Ann Intern Med 1999;130(6):478–86.
11. Nepom GT, Byers P, Seyfried C, Healey LA, Wilske KR, Stage D, et al. HLA genes associated with rheumatoid arthritis. Identification of susceptibility alleles using specific oligonucleotide probes. Arthritis Rheum 1989;32(1):15–21.
12. Gao XJ, Olsen NJ, Pincus T, Stastny P. HLA-DR alleles with naturally occurring amino acid substitutions and risk for development of rheumatoid arthritis. Arthritis Rheum 1990;33(7):939–46.
13. Nakai Y, Wakisaka A, Aizawa M, Itakura K, Nakai H, Ohashi A. HLA and rheumatoid arthritis in the Japanese. Arthritis Rheum 1981;24(5):722–5.
14. Ohta N, Nishimura YK, Tanimoto K, Horiuchi Y, Abe C, Shiokawa Y, et al. Association between HLA and Japanese patients with rheumatoid arthritis. Hum Immunol 1982;5(2):123–32.
15. Fox DA. The role of T cells in the immunopathogenesis of rheumatoid arthritis: new perspectives. Arthritis Rheum 1997;40(4):598–609.
16. Goronzy JJ, Weyand CM. T-cell regulation in rheumatoid arthritis. Curr Opin Rheumatol 2004;16(3):212–7.
17. Gracie JA, Forsey RJ, Chan WL, Gilmour A, Leung BP, Greer MR, et al. A proinflammatory role for IL-18 in rheumatoid arthritis. J Clin Invest 1999;104(10):1393–401.
18. Qin S, Rottman JB, Myers P, Kassam N, Weinblatt M, Loetscher M, et al. The chemokine receptors CXCR3 and CCR5 mark subsets of T cells associated with certain inflammatory reactions. J Clin Invest 1998;101(4):746–54.
19. Eguchi K, Ueki Y, Shimomura C, Otsubo T, Nakao H, Migita K, et al. Increment in the Tal+ cells in the peripheral blood and thyroid tissue of patients with Graves' disease. J Immunol 1989;142(12):4233–40.
20. Gerli R, Muscat C, Bertotto A, Bistoni O, Agea E, Tognellini R, et al. CD26 surface molecule involvement in T-cell activation and lymphokine synthesis in rheumatoid and other inflammatory synovitis. Clin Immunol Immunopathol 1996;80(1):31–7.
21. Hafler DA, Fox DA, Manning ME, Schlossman SF, Reinherz EL, Weiner HL. In vivo activated T lymphocytes in the peripheral blood and cerebrospinal fluid of patients with multiple sclerosis. N Engl J Med 1985;312(22):1405–11.
22. Mizokami A, Eguchi K, Kawakami A, Ida H, Kawabe Y, Tsukada T, et al. Increased population of high fluorescence 1F7 (CD26) antigen on T cells in synovial fluid of patients with rheumatoid arthritis. J Rheumatol 1996;23(12):2022–6.
23. Muscat C, Bertotto A, Agea E, Bistoni O, Ercolani R, Tognellini R, et al. Expression and functional role of 1F7 (CD26) antigen on peripheral blood and synovial fluid T cells in rheumatoid arthritis patients. Clin Exp Immunol 1994;98(2):252–6.
24. Masuyama J, Berman JS, Cruikshank WW, Morimoto C, Center DM. Evidence for recent as well as long term activation of T cells migrating through endothelial cell monolayers in vitro. J Immunol 1992;148(5):1367–74.
25. Appleman LJ, Boussiotis VA. T cell anergy and costimulation. Immunol Rev 2003;192:161–80.
26. Dang NH, Torimoto Y, Shimamura K, Tanaka T, Daley JF, Schlossman SF, et al. 1F7 (CD26): a marker of thymic maturation involved in the differential regulation of the CD3 and CD2 pathways of human thymocyte activation. J Immunol 1991;147(9):2825–32.
27. Dang NH, Torimoto Y, Sugita K, Daley JF, Schow P, Prado C, et al. Cell surface modulation of CD26 by anti-1F7 monoclonal antibody. Analysis of surface expression and human T cell activation. J Immunol 1990;145(12):3963–71.
28. Morimoto C, Schlossman SF. The structure and function of CD26 in the T-cell immune response. Immunol Rev 1998;161:55–70.
29. Morimoto C, Torimoto Y, Levinson G, Rudd CE, Schrieber M, Dang NH, et al. 1F7, a novel cell surface molecule, involved in helper function of CD4 cells. J Immunol 1989;143(11):3430–9.
30. Ohnuma K, Munakata Y, Ishii T, Iwata S, Kobayashi S, Hosono O, et al. Soluble CD26/dipeptidyl peptidase IV induces T cell proliferation through CD86 up-regulation on APCs. J Immunol 2001;167(12):6745–55.
31. Ohnuma K, Yamochi T, Uchiyama M, Nishibashi K, Yoshikawa N, Shimizu N, et al. CD26 up-regulates expression of CD86 on antigen-presenting cells by means of caveolin-1. Proc Natl Acad Sci USA 2004;101(39):14186–91.
32. Tanaka T, Camerini D, Seed B, Torimoto Y, Dang NH, Kameoka J, et al. Cloning and functional expression of the T cell activation antigen CD26. J Immunol 1992;149(2):481–6.
33. Naquet P, MacDonald HR, Brekelmans P, Barbet J, Marchetto S, Van Ewijk W, et al. A novel T cell-activating molecule (THAM) highly expressed on CD4-CD8- murine thymocytes. J Immunol 1988;141(12):4101–9.

34. Yan S, Marguet D, Dobers J, Reutter W, Fan H. Deficiency of CD26 results in a change of cytokine and immunoglobulin secretion after stimulation by pokeweed mitogen. Eur J Immunol 2003;33(6):1519–27.
35. Marguet D, Baggio L, Kobayashi T, Bernard AM, Pierres M, Nielsen PF, et al. Enhanced insulin secretion and improved glucose tolerance in mice lacking CD26. Proc Natl Acad Sci USA 2000;97(12):6874–9.
36. Fleischer B. CD26: a surface protease involved in T-cell activation. Immunol Today 1994;15(4):180–4.
37. von Bonin A, Huhn J, Fleischer B. Dipeptidyl-peptidase IV/CD26 on T cells: analysis of an alternative T-cell activation pathway. Immunol Rev 1998;161:43–53.
38. Oravecz T, Pall M, Roderiquez G, Gorrell MD, Ditto M, Nguyen NY, et al. Regulation of the receptor specificity and function of the chemokine RANTES (regulated on activation, normal T cell expressed and secreted) by dipeptidyl peptidase IV (CD26)-mediated cleavage. J Exp Med 1997;186(11):1865–72.
39. Proost P, Struyf S, Schols D, Opdenakker G, Sozzani S, Allavena P, et al. Truncation of macrophage-derived chemokine by CD26/dipeptidyl-peptidase IV beyond its predicted cleavage site affects chemotactic activity and CC chemokine receptor 4 interaction. J Biol Chem 1999;274(7):3988–93.
40. Christopherson KW, 2nd, Hangoc G, Mantel CR, Broxmeyer HE. Modulation of hematopoietic stem cell homing and engraftment by CD26. Science 2004;305(5686):1000–3.
41. Christopherson KW, Cooper S, Hangoc G, Broxmeyer HE. CD26 is essential for normal G-CSF-induced progenitor cell mobilization as determined by CD26-/- mice. Exp Hematol 2003;31(11):1126–34.
42. Christopherson KW, 2nd, Hangoc G, Broxmeyer HE. Cell surface peptidase CD26/dipeptidylpeptidase IV regulates CXCL12/stromal cell-derived factor-1 alpha-mediated chemotaxis of human cord blood CD34+ progenitor cells. J Immunol 2002;169(12):7000–8.
43. Wiedeman PE, Trevillyan JM. Dipeptidyl peptidase IV inhibitors for the treatment of impaired glucose tolerance and type 2 diabetes. Curr Opin Invest Drugs 2003;4(4):412–20.
44. Ristic S, Byiers S, Foley J, Holmes D. Improved glycaemic control with dipeptidyl peptidase-4 inhibition in patients with type 2 diabetes: vildagliptin (LAF237) dose response. Diabetes Obes Metab 2005;7(6):692–8.
45. Dang NH, Torimoto Y, Deusch K, Schlossman SF, Morimoto C. Comitogenic effect of solid-phase immobilized anti-1F7 on human CD4 T cell activation via CD3 and CD2 pathways. J Immunol 1990;144(11):4092–100.
46. Dang NH, Torimoto Y, Schlossman SF, Morimoto C. Human CD4 helper T cell activation: functional involvement of two distinct collagen receptors, 1F7 and VLA integrin family. J Exp Med 1990;172(2):649–52.
47. Ruiz P, Zacharievich N, Hao L, Viciana AL, Shenkin M. Human thymocyte dipeptidyl peptidase IV (CD26) activity is altered with stage of ontogeny. Clin Immunol Immunopathol 1998;88(2):156–68.
48. Tanaka T, Kameoka J, Yaron A, Schlossman SF, Morimoto C. The costimulatory activity of the CD26 antigen requires dipeptidyl peptidase IV enzymatic activity. Proc Natl Acad Sci USA 1993;90(10):4586–90.
49. Kameoka J, Tanaka T, Nojima Y, Schlossman SF, Morimoto C. Direct association of adenosine deaminase with a T cell activation antigen, CD26. Science 1993;261(5120):466–9.
50. Dong RP, Kameoka J, Hegen M, Tanaka T, Xu Y, Schlossman SF, et al. Characterization of adenosine deaminase binding to human CD26 on T cells and its biologic role in immune response. J Immunol 1996;156(4):1349–55.
51. Dong RP, Tachibana K, Hegen M, Munakata Y, Cho D, Schlossman SF, et al. Determination of adenosine deaminase binding domain on CD26 and its immunoregulatory effect on T cell activation. J Immunol 1997;159(12):6070–6.
52. Goldblum RM, Schmalstieg FC, Nelson JA, Mills GC. Adenosine deaminase (ADA) and other enzyme abnormalities in immune deficiency states. Birth Defects Orig Artic Ser 1978;14(6A):73–84.
53. Dang NH, Hagemeister FB, Duvic M, Romaguera JE, Younes A, Jones D, et al. Pentostatin in T-non-Hodgkin's lymphomas: efficacy and effect on CD26+ T lymphocytes. Oncol Rep 2003; 10(5):1513–8.
54. Torimoto Y, Dang NH, Vivier E, Tanaka T, Schlossman SF, Morimoto C. Coassociation of CD26 (dipeptidyl peptidase IV) with CD45 on the surface of human T lymphocytes. J Immunol 1991;147(8):2514–7.
55. Ishii T, Ohnuma K, Murakami A, Takasawa N, Kobayashi S, Dang NH, et al. CD26-mediated signaling for T cell activation occurs in lipid rafts through its association with CD45RO. Proc Natl Acad Sci USA 2001;98(21):12138–43.
56. Kobayashi S, Ohnuma K, Uchiyama M, Iino K, Iwata S, Dang NH, et al. Association of CD26 with CD45RA outside lipid rafts attenuates cord blood T-cell activation. Blood 2004;103(3):1002–10.
57. Iwaki-Egawa S, Watanabe Y, Kikuya Y, Fujimoto Y. Dipeptidyl peptidase IV from human serum: purification, characterization, and N-terminal amino acid sequence. J Biochem (Tokyo) 1998;124(2):428–33.
58. Durinx C, Lambeir AM, Bosmans E, Falmagne JB, Berghmans R, Haemers A, et al. Molecular characterization of dipeptidyl peptidase activity in serum: soluble CD26/dipeptidyl peptidase IV is responsible for the release of X-Pro dipeptides. Eur J Biochem 2000;267(17):5608–13.
59. Tanaka T, Duke-Cohan JS, Kameoka J, Yaron A, Lee I, Schlossman SF, et al. Enhancement of antigen-induced T-cell proliferation by soluble CD26/dipeptidyl peptidase IV. Proc Natl Acad Sci USA 1994;91(8):3082–6.
60. Glenney JR Jr. Tyrosine phosphorylation of a 22-kDa protein is correlated with transformation by Rous sarcoma virus. J Biol Chem 1989;264(34):20163–6.
61. Rothberg KG, Heuser JE, Donzell WC, Ying YS, Glenney JR, Anderson RG. Caveolin, a protein component of caveolae membrane coats. Cell 1992;68(4):673–82.
62. Yamada E. The fine structure of the gall bladder epithelium of the mouse. J Biophys Biochem Cytol 1955;1(5):445–58.
63. Smart EJ, Graf GA, McNiven MA, Sessa WC, Engelman JA, Scherer PE, et al. Caveolins, liquid-ordered domains, and signal transduction. Mol Cell Biol 1999;19(11):7289–304.
64. Razani B, Engelman JA, Wang XB, Schubert W, Zhang XL, Marks CB, et al. Caveolin-1 null mice are viable but show evidence of hyperproliferative and vascular abnormalities. J Biol Chem 2001;276(41):38121–38.
65. Razani B, Wang XB, Engelman JA, Battista M, Lagaud G, Zhang XL, et al. Caveolin-2-deficient mice show evidence of severe pulmonary dysfunction without disruption of caveolae. Mol Cell Biol 2002;22(7):2329–44.
66. Galbiati F, Engelman JA, Volonte D, Zhang XL, Minetti C, Li M, et al. Caveolin-3 null mice show a loss of caveolae, changes in the microdomain distribution of the dystrophin-glycoprotein complex, and t-tubule abnormalities. J Biol Chem 2001;276(24):21425–33.
67. Scherer PE, Okamoto T, Chun M, Nishimoto I, Lodish HF, Lisanti MP. Identification, sequence, and expression of caveolin-2 defines a caveolin gene family. Proc Natl Acad Sci USA 1996;93(1):131–5.
68. Scherer PE, Tang Z, Chun M, Sargiacomo M, Lodish HF, Lisanti MP. Caveolin isoforms differ in their N-terminal protein sequence and subcellular distribution. Identification and epitope mapping of an isoform-specific monoclonal antibody probe. J Biol Chem 1995;270(27):16395–401.
69. Couet J, Li S, Okamoto T, Ikezu T, Lisanti MP. Identification of peptide and protein ligands for the caveolin-scaffolding domain. Implications for the interaction of caveolin with caveolae-associated proteins. J Biol Chem 1997;272(10):6525–33.
70. Gargalovic P, Dory L. Caveolins and macrophage lipid metabolism. J Lipid Res 2003;44(1):11–21.
71. Riemann D, Hansen GH, Niels-Christiansen L, Thorsen E, Immerdal L, Santos AN, et al. Caveolae/lipid rafts in fibroblast-like synoviocytes: ectopeptidase-rich membrane microdomains. Biochem J 2001;354(Pt 1):47–55.
72. Woodman SE, Ashton AW, Schubert W, Lee H, Williams TM, Medina FA, et al. Caveolin-1 knockout mice show an impaired angiogenic response to exogenous stimuli. Am J Pathol 2003; 162(6):2059–68.
73. Liu J, Wang XB, Park DS, Lisanti MP. Caveolin-1 expression enhances endothelial capillary tubule formation. J Biol Chem 2002;277(12):10661–8.

74. Bucci M, Gratton JP, Rudic RD, Acevedo L, Roviezzo F, Cirino G, et al. In vivo delivery of the caveolin-1 scaffolding domain inhibits nitric oxide synthesis and reduces inflammation. Nat Med 2000; 6(12):1362–7.
75. Cheng HC, Abdel-Ghany M, Elble RC, Pauli BU. Lung endothelial dipeptidyl peptidase IV promotes adhesion and metastasis of rat breast cancer cells via tumor cell surface-associated fibronectin. J Biol Chem 1998;273(37):24207–15.
76. Cheng HC, Abdel-Ghany M, Pauli BU. A novel consensus motif in fibronectin mediates dipeptidyl peptidase IV adhesion and metastasis. J Biol Chem 2003;278(27):24600–7.
77. Wrenger S, Faust J, Mrestani-Klaus C, Fengler A, Stockel-Maschek A, Lorey S, et al. Down-regulation of T cell activation following inhibition of dipeptidyl peptidase IV/CD26 by the N-terminal part of the thromboxane A2 receptor. J Biol Chem 2000;275(29):22180–6.
78. Herrera C, Morimoto C, Blanco J, Mallol J, Arenzana F, Lluis C, et al. Comodulation of CXCR4 and CD26 in human lymphocytes. J Biol Chem 2001;276(22):19532–9.
79. Montesano R, Roth J, Robert A, Orci L. Non-coated membrane invaginations are involved in binding and internalization of cholera and tetanus toxins. Nature 1982;296(5858):651–3.
80. Pelkmans L, Helenius A. Endocytosis via caveolae. Traffic 2002; 3(5):311–20.
81. Grakoui A, Bromley SK, Sumen C, Davis MM, Shaw AS, Allen PM, et al. The immunological synapse: a molecular machine controlling T cell activation. Science 1999;285(5425):221–7.
82. Turley SJ, Inaba K, Garrett WS, Ebersold M, Unternaehrer J, Steinman RM, et al. Transport of peptide-MHC class II complexes in developing dendritic cells. Science 2000;288(5465):522–7.
83. Brennan FM, Hayes AL, Ciesielski CJ, Green P, Foxwell BM, Feldmann M. Evidence that rheumatoid arthritis synovial T cells are similar to cytokine-activated T cells: involvement of phosphatidylinositol 3-kinase and nuclear factor kappaB pathways in tumor necrosis factor alpha production in rheumatoid arthritis. Arthritis Rheum 2002;46(1):31–41.
84. Kremer JM, Westhovens R, Leon M, Di Giorgio E, Alten R, Steinfeld S, et al. Treatment of rheumatoid arthritis by selective inhibition of T-cell activation with fusion protein CTLA4Ig. N Engl J Med 2003;349(20):1907–15.
85. Moreland LW, Alten R, Van den Bosch F, Appelboom T, Leon M, Emery P, et al. Costimulatory blockade in patients with rheumatoid arthritis: a pilot, dose-finding, double-blind, placebo-controlled clinical trial evaluating CTLA-4Ig and LEA29Y eighty-five days after the first infusion. Arthritis Rheum 2002;46(6): 1470–9.
86. Lindsten T, Lee KP, Harris ES, Petryniak B, Craighead N, Reynolds PJ, et al. Characterization of CTLA-4 structure and expression on human T cells. J Immunol 1993;151(7):3489–99.
87. Freeman GJ, Gribben JG, Boussiotis VA, Ng JW, Restivo VA Jr, Lombard LA, et al. Cloning of B7-2: a CTLA-4 counter-receptor that costimulates human T cell proliferation. Science 1993; 262(5135):909–11.
88. Brunet JF, Denizot F, Luciani MF, Roux-Dosseto M, Suzan M, Mattei MG, et al. A new member of the immunoglobulin superfamily - CTLA-4. Nature 1987;328(6127):267–70.
89. Linsley PS, Greene JL, Brady W, Bajorath J, Ledbetter JA, Peach R. Human B7-1 (CD80) and B7-2 (CD86) bind with similar avidities but distinct kinetics to CD28 and CTLA-4 receptors. Immunity 1994;1(9):793–801.
90. Freeman GJ, Borriello F, Hodes RJ, Reiser H, Hathcock KS, Laszlo G, et al. Uncovering of functional alternative CTLA-4 counter-receptor in B7-deficient mice. Science 1993;262(5135): 907–9.

Oncogene (2005) 24, 1262–1271

www.nature.com/onc

HTLV-I Tax induces and associates with Crk-associated substrate lymphocyte type (Cas-L)

Satoshi Iwata[1], Akiko Souta-Kuribara[1], Akio Yamakawa[2], Takahiro Sasaki[1], Takatsune Shimizu[3], Osamu Hosono[1], Hiroshi Kawasaki[1], Hirotoshi Tanaka[1], Nam H Dang[4], Toshiki Watanabe[5], Naomichi Arima[6] and Chikao Morimoto*,[1]

[1]*Division of Clinical Immunology, Advanced Clinical Research Center, Institute of Medical Science, The University of Tokyo, 4-6-1 Shirokanedai, Minato-ku, Tokyo 108-8639, Japan;* [2]*Department of Cancer Biology, Dana-Farber Cancer Institute, Harvard Medical School, 44 Binney Street, Boston, MA 02115, USA;* [3]*Department of Internal Medicine, Keio University School of Medicine, 35 Shinanomachi, Shinjyuku-ku, Tokyo 160-8582, Japan;* [4]*Department of LymphomalMyeloma UT, MD Anderson Cancer Center, Houston, TX 77030, USA;* [5]*Laboratory of Tumor Cell Biology, Department of Medical Genome Sciences, Graduate School of Frontier Sciences, The University of Tokyo, 4-6-1 Shirokanedai, Minato-ku, Tokyo 108-8639, Japan;* [6]*Division of Host Response, Center for Chronic Viral Diseases, Faculty of Medicine, Kagoshima University, 8-35-1 Sakuragaoka, Kagoshima 890-8520, Japan*

Crk-associated substrate lymphocyte type (Cas-L) is a docking protein that is heavily tyrosine phosphorylated by the engagement of β1 integrins in T cells. In the present study, we attempted to evaluate the role of Cas-L in the pathophysiology of adult T-cell leukemia (ATL). Examination of peripheral blood mononuclear cells from ATL patients as well as ATL-derived T cell lines showed an elevation of Cas-L in these cells. We showed that tyrosine phosphorylation as well as expression of Cas-L was markedly elevated through the induction of human T-lymphotropic virus type I (HTLV-I) Tax in JPX-9 cells, with these cells showing marked motile behavior on the ligands for integrins. We next performed yeast two-hybrid screening of cDNA library from an HTLV-I-transformed T cell line, which resulted in the identification of Tax as a putative binding partner for Cas-L. Co-precipitation experiments revealed that the serine-rich region of Cas-L might serve as the binding site with the highest affinity for Tax. Co-localization study showed that Tax and Cas-L partly merged in the cytoplasm. Finally, we showed that exogenous Cas-L inhibited Tax-mediated transactivation of nuclear factor κB (NF-κB), while Tax-independent activation of NF-κB remained intact, hence indicating that Cas-L might specifically regulate Tax-NF-κB pathway.

Oncogene (2005) **24**, 1262–1271. doi:10.1038/sj.onc.1208261
Published online 13 December 2004

Keywords: ATL; Tax; HTLV-I; NF-κB; Cas-L; HEF1

Introduction

It has been shown that β1 integrins exhibit a variety of biological functions such as cytokine production, proliferation, cell differentiation, cell survival, apoptosis, and cell migration as well as cell adhesion through specific interaction with their ligands (extracellular matrix and vascular cell adhesion molecule (VCAM)-1) (Hemler, 1990; Hynes, 1992; Juliano and Haskill, 1993; Ruoslahti and Reed, 1994). To understand the molecular mechanisms involved with these numerous biological effects, it is particularly important to analyse cell signaling through the β1 integrins. In this regard, we demonstrated that interaction of FN and very late antigen (VLA)-5 or the CS-1 domain of FN and VLA-4 could induce costimulatory signals to CD3/TCR pathway (Matsuyama *et al.*, 1989; Nojima *et al.*, 1990). Our subsequent study showed that PLC-γ, FAK (focal adhesion kinase), paxillin, fyn, lck, ERK1/2, and pp105 were tyrosine-phosphorylated upon engagement of β1 integrins in T cells (Nojima *et al.*, 1992; Sato *et al.*, 1995; Tachibana *et al.*, 1995). Isolation of cDNA encoding pp105 revealed that this protein belonged to Cas family, and we designated it Cas-L (Cas lymphocyte type) (Law *et al.*, 1996; Minegishi *et al.*, 1996).

Cas-L is a docking protein that is heavily tyrosine phosphorylated by FAK and Src family kinases upon engagement of β1 integrins as well as the TCR complex in T cells (Tachibana *et al.*, 1997; Ohashi *et al.*, 1998). Cas-L cDNA was cloned initially from adult T-cell leukemia (ATL)-derived T cell lines, and its expression was markedly elevated in those cells (Minegishi *et al.*, 1996). Recently, we have demonstrated that Cas-L was overexpressed and tyrosine phosphorylated *in vivo* in human T-lymphotropic virus type I (HTLV-I) Tax transgenic mice (Miyake-Nishijima *et al.*, 2003). These facts led us to evaluate the possible biological link among Cas-L, Tax, and HTLV-I-related disorders.

It is known that HTLV-I is the etiologic agent for ATL (Uchiyama *et al.*, 1977; Yodoi and Uchiyama, 1986; Yoshida, 1993). One of the characteristics of this malignancy is the infiltration of leukemic T cells into the skin and other organs. Although the precise mechanism of pathogenesis of ATL remains unclear, $p40^{tax}$ protein is thought to play a key role in HTLV-I-mediated

*Correspondence: C Morimoto; E-mail: morimoto@ims.u-tokyo.ac.jp
Received 8 March 2004; revised 16 September 2004; accepted 1 October 2004; published online 13 December 2004

transformation of T cells (Yoshida, 1993). Tax, encoded by the pX region of the HTLV-I genome, is a potent transactivator of various host genes as well as HTLV-I LTR-mediated transcription of the viral genome (Sodroski *et al.*, 1984). Tax activates transcription of numerous host cellular genes associated with lymphocyte proliferation, for examples, proto-oncogenes (Fujii *et al.*, 1991), cytokines and cytokine receptors including IL-2R (Inoue *et al.*, 1986; Maruyama *et al.*, 1987; Cross *et al.*, 1987), c-fos (Fujii *et al.*, 1988; Nagata *et al.*, 1989), TGF-β (Kim *et al.*, 1990), gp34/OX-40/CD134 (Miura *et al.*, 1991), IL-6 (Yamashita *et al.*, 1994), TNF-α (Albrecht *et al.*, 1992), IL-8 (Mori *et al.*, 1998), as well as the integrated provirus of HTLV-I (Sodroski *et al.*, 1984). These findings suggest its close association with T-cell immortalization and transformation. It has been shown that this transactivation of host genes is mediated through the interaction of $p40^{tax}$ with several cellular transcription factors, such as cyclic AMP-responsive element binding protein/activating transcriptional factor (CREB/ATF), NF-κB, and serum responsive factor (SRF) (Yoshimura *et al.*, 1990; Yoshida, 1993; Franchini, 1995; Harhaj and Sun, 1999).

In this paper, we demonstrate the possible involvement of Cas-L in the pathogenesis of ATL through Tax-mediated overexpression and hyper-phosphorylation of Cas-L, which resulted in markedly enhanced motility of lymphocytes. Furthermore, we showed that the interaction of Tax and Cas-L may result in the modulation of Tax-mediated transactivation of NF-κB.

Results

Predominant expression of Cas-L in HTLV-I-transformed T cell lines and ATL-derived T cell lines

We previously described and cloned pp105/Cas-L in ATL-derived T cell lines H9 (Nojima *et al.*, 1992; Minegishi *et al.*, 1996). In those cells, higher levels of Cas-L protein and mRNA were observed than unstimulated peripheral T cells. To investigate the distribution of Cas-L, a variety of HTLV-I-transformed T cell lines, ATL-derived T cell lines, and HTLV-I-unrelated T cell lines were examined for expression of Cas-L as well as FAK, Pyk2 (FAK-related tyrosine kinase), paxillin, and HTLV-I Tax. As shown in Figure 1, the expression of Cas-L was higher in the cases of HTLV-I-transformed T cell lines (MT-1, MT-2, and MT-4) and ATL-derived T cell lines (Hut-102, H9, and SLB-I) than HTLV-I-unrelated T cell lines (Jurkat and HPB-ALL). In contrast, expression of FAK, Pyk2, and paxillin, which are also involved in β1 integrin-mediated cell signaling, did not exhibit such distribution pattern among these T cell lines.

Elevation in protein level and tyrosine phosphorylation level of Cas-L and other related signal-transducing proteins downstream of β1 integrins in Tax-induced JPX-9 cells

Since our results showed that ATL-derived and HTLV-I transformed T cell lines expressed Cas-L at higher levels,

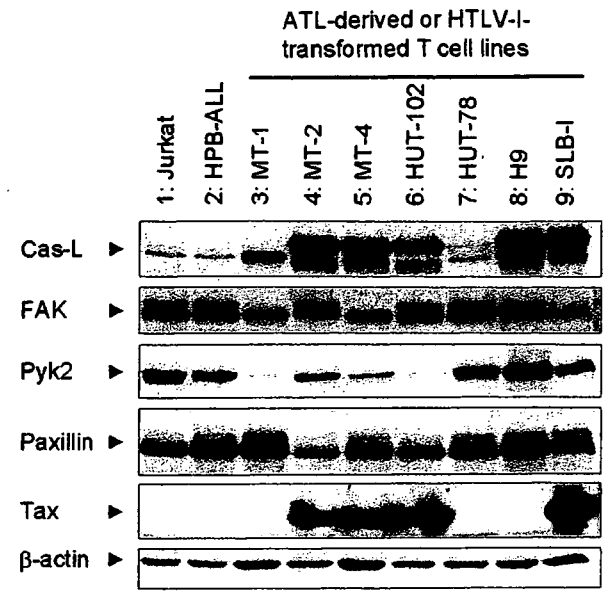

Figure 1 Expression of Cas-L in ATL-derived or HTLV-I-transformed T cell line and HTLV-I (−) T cell lines. Each indicated cell line was lysed in 1% NP-40 lysis buffer. Equal amounts of the whole-cell lysates (50 μg per lane) were separated on SDS–PAGE, and analysed by immunoblotting with anti-Cas mAb, anti-FAK mAb, anti-Pyk2 mAb, anti-paxillin mAb, anti-Tax mAb, and anti-β-actin mAb, respectively

we hypothesize that HTLV-I Tax protein might cause the preferential overproduction of Cas-L in HTLV-I-infected T cell lines. We examined the expression of Cas-L in JPX-9 cells and JPX-M cells, in which Tax protein is induced by a metallothionein promoter (Nagata *et al.*, 1989). JPX-M cells were used as negative controls, in which inactive mutant Tax protein was induced by the same stimuli. As shown in Figure 2a, Cas-L protein level was elevated in JPX-9 cells in a time-dependent manner after the addition of $CdCl_2$, whereas control JPX-M cells stimulated in the same condition did not show any alteration in Cas-L level.

We next compared the expression of Cas-L and other proteins involved in β1 integrin-mediated signaling by immunoprecipitation and immunoblotting. As shown in Figure 2b, the levels of FAK, paxillin, and Cas-L were also elevated following induction of Tax in JPX-9 cells. Surprisingly, levels of spontaneous tyrosine phosphorylation of Cas-L, FAK, Pyk2, and paxillin were also elevated by induction of Tax. In contrast, the levels of protein expression and tyrosine phosphorylation of these proteins were not altered in JPX-M cells.

Enhanced motility of Tax-induced JPX-9 cells

We previously reported that gene transfer of Cas-L provided Jurkat cells with motile behavior on FN-, CD3- plus FN-, and CS-1-coated surface, and that this enhancement of motility required the tyrosine phosphorylation of Cas-L (Ohashi *et al.*, 1999). We therefore evaluated the motility of JPX-9 cells and JPX-M cells on CS-1-coated Transwell™ insert. As shown in Figure 3a,

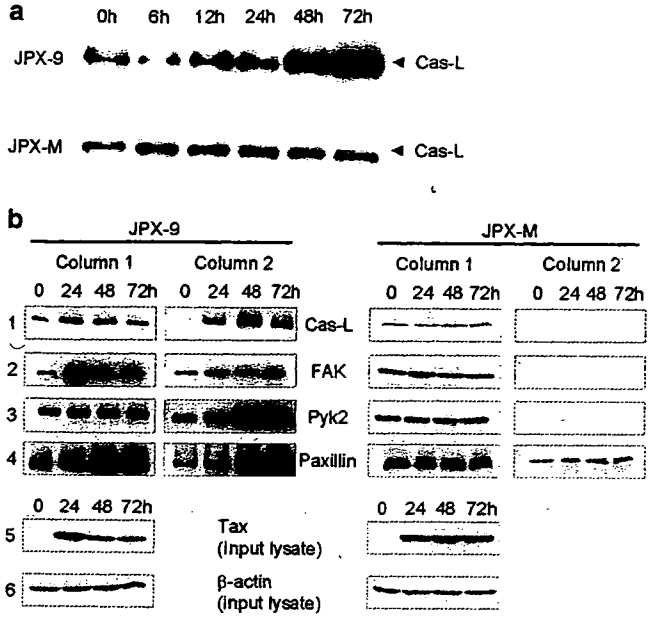

Figure 2 (a) Cas-L induction by $CdCl_2$ in JPX-9 cells. JPX-9 cells and JPX-M cells were cultured in the presence of 10 μM $CdCl_2$ at 37°C for 6–72 h. Equal amounts of the whole-cell lysates (50 μg per lane) were separated on SDS–PAGE, and analysed by immunoblotting with anti-Cas mAb. (b) Protein amounts of Cas-L, FAK, Pyk2 and paxillin and their levels of tyrosine phosphorylation in Tax-induced JPX-9 cells and JPX-M cells. JPX-9 cells and JPX-M cells were cultured in the presence of 10 μM $CdCl_2$ at 37°C for 24–72 h. In total, 1×10^7 cells were lysed in the 1% NP-40 lysis buffer and immunoprecipitated with anti-Cas-L Ab, anti-FAK mAb, anti-Pyk2 mAb, or anti-paxillin mAb, respectively. The precipitates were analysed by immunoblotting with anti-Cas mAb, anti-FAK mAb, anti-Pyk2 mAb, or anti-paxillin mAb, and reprobed with anti-phosphotyrosine mAb (4G10; pTyr)

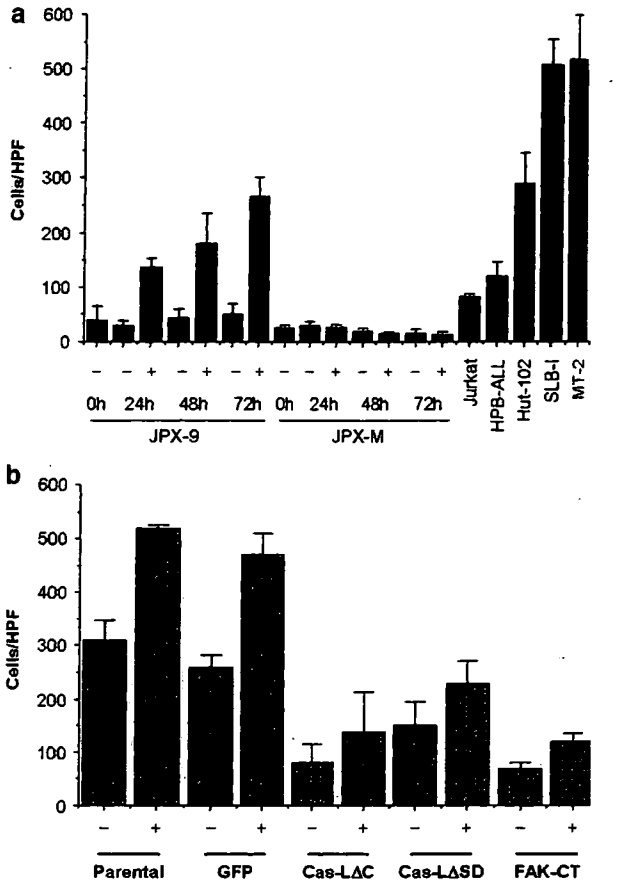

Figure 3 (a) Tax-induced cell motility on CS-1 in JPX-9 cells and JPX-M cells. JPX-9 cells and JPX-M cells were cultured with or without 10 μM of $CdCl_2$ at 37°C for 24–72 h. Jurkat, HPB-ALL, Hut-102, SLB-I, and MT-2 cells were cultured in normal medium and harvested prior to the assay. The cells were incubated at 37°C for 4 h on the Transwell™ inserts coated with CS-1/GST fusion protein (5 μg/ml). (b) Tax-induced cell motility on FN and CD3 mAb in JPX-9 cells infected with retrovirus coding for dominant-negative constructs of Cas-L or FAK. JPX-9 cells and those infected with each retrovirus (GFP: pMX-IRES-GFP, ΔC: pMX-Cas-LΔC-IRES-GFP, ΔSD: pMX-Cas-LΔSD-IRES-GFP, FAKCT: pMX-FAKCT-IRES-GFP) were cultured in the presence or absence of $CdCl_2$ for 48 h. Cells were incubated at 37°C for 4 h on the Transwell™ inserts coated with FN and CD3 mAb (5 μg/ml each). Data are representative of two independent experiments (a, b)

JPX-9 cells stimulated with $CdCl_2$ displayed remarkable motility compared to unstimulated JPX-9 cells. In the control JPX-M cells, such promotion of motility by induction of Tax was not observed. As shown in the figure, the enhanced motility observed in Tax-induced JPX-9 cells was comparable to Hut-102, SLB-I, and MT-2, which showed higher motility than HTLV-I-unrelated T cell lines (Jurkat and HPB-ALL). To further characterize the cell motility observed in the Tax- and Cas-L induced JPX-9 cells, we transduced dominant-negative Cas-L (ΔSD and ΔC) or FAK-CT constructs by retroviral gene transfer. As shown in Figure 3b, gene transfer of these constructs resulted in the reduced induction of motility on CD3 plus FN-coated surface, indicating that Tax-mediated enhancement of T cell motility was at least partly mediated through β1 integrins–Cas-L pathway.

Enhanced expression and tyrosine phosphorylation of Cas-L in PBMCs from ATL patients

To further explore the clinical relevance of Cas-L overproduction in HTLV-I-related diseases, we obtained samples from ATL patients as well as asymptomatic HTLV-I carriers. As shown in Figure 4, mononuclear cells from the peripheral blood of ATL patients had elevated expression of Cas-L in four of five cases examined. Interestingly, the levels of tyrosine phosphorylation of Cas-L were clearly elevated in two of those cases (#4 and #8). In contrast, neither overproduction of Cas-L nor enhanced phosphorylation of Cas-L was observed in the cases with asymptomatic HTLV-I carriers. Thus, overproduction of Cas-L and, in some cases, elevation of its tyrosine phosphorylation was also observed in ATL patients.

Identification of Tax as a putative Cas-L binding protein

To further understand the biological significance of Cas-L in ATL and HTLV-I related disorders, we next performed two-hybrid cDNA cloning in search for Cas-L binding proteins. We screened over 1×10^6 indepen-

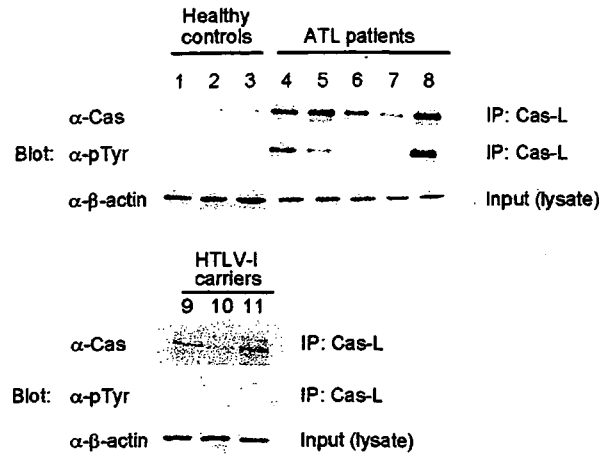

Figure 4 Expression and tyrosine phosphorylation of Cas-L in PBMCs from ATL patients and HTLV-I carriers. Leukemic cells from five patients diagnosed with acute-type ATL (lanes 4–8), and PBMCs from HTLV-I infected individuals (lanes 9–11) and healthy controls (lanes 1–3) were analysed. The diagnosis of ATL and HTLV-I carrier was based on clinical features, hematologic findings, and the presence of anti-HTLV-I antibodies in patient sera. Equal amounts of the whole-cell lysates (25 μg per lane) were separated on SDS–PAGE, and analysed by immunoblotting with anti-Cas mAb (α-Cas; the upper panel), then reprobed with anti-phosphotyrosine mAb (α-pTyr; the middle panel). As controls, immunoblotting with anti-β-actin mAb was carried out (α-β-actin; the bottom panel)

dent clones from the cDNA library of an HTLV-I infected T cell line, SLB-I. Among 180 clones selected by histidine prototrophy and β-Gal expression, we were especially interested in two independent Tax clones, one (clone #80) of which contained almost full-length (aa 2–353) Tax and the other (clone #45) of which contained the c-terminal half (aa 192–353) of the Tax cDNA in frame.

Co-precipitation of Cas-L and p130Cas with Tax

To evaluate protein–protein interaction of Cas-L and Tax, we performed co-precipitation experiments using 293T cells. Initially, we employed full-length constructs for Cas-L and p130Cas, another Cas family member. As shown in Figure 5a, transfected Cas-L was co-precipitated with Tax in those cells. Since p130Cas was the first reported Cas family protein with well-conserved domain structures, we performed the same studies as those done with Cas-L, and found that p130Cas was similarly co-precipitated with Tax.

We also performed the co-precipitation experiments using MT-2 and Hut-102 cells that co-express Cas-L and Tax. As shown in Figure 5b, Cas-L protein was co-precipitated with Tax in those cells, suggesting that endogenous Cas-L and Tax associated with each other in HTLV-I-infected T cell lines.

Determination of Tax-binding domains of Cas-L

To identify the Tax-binding domain of Cas-L, we first employed a series of deletion mutants: Cas-LΔSH3: lacking SH3 domain (aa 1–60); ΔSD: lacking substrate domain (aa 63–401); and ΔC: lacking c-terminal half (aa 406–834). We also prepared a point mutant Cas-LF, in which the Src-SH2-binding motif YDYVHL was mutated to FDFVHL (Tachibana *et al.*, 1997). The structures of these mutants were schematically summarized in Figure 5c. Unexpectedly, none of these mutations or deletions could abolish the binding capability of Cas-L with Tax in 293T cells (Figure 5d), implying multiple binding sites were present in Cas-L, as was suggested in the case involving the association of Cas-L/HEF1 and Smad3 (Liu *et al.*, 2000). We then produced GST-fusion protein of each domain. As shown in Figure 5e, SR or SRF had equivalent and the strongest binding capability. In addition, SD and HLH showed significant binding with Tax, whereas SH3 showed no binding capability.

Co-localization of Cas-L with Tax in the cytosol of transfected 293T, MT-2, and Hut-102 cells

We next determined the co-localization of Cas-L with Tax by confocal microscopy. As shown in Figure 6A, transfected c-myc-tagged Cas-L alone mainly localized in the cytosol (column a, row 2), which was not altered by the co-transfection of Tax (column a, row 1). In contrast, transfected Tax localized both in the nucleus and cytosol (nucleus dominant; column b, row 3), which was changed to a cytosol dominant pattern (column b, row 2). This alteration of subcellular localization was observed especially in cells co-expressing Cas-L and Tax (column c, row 1). Furthermore, Cas-L and Tax were mainly co-localized in the cytosol (column c, row 1). Similar results were also observed in the cases with Hut-102 and MT-2 cells, in which Cas-L and Tax proteins were endogenously co-expressed (Figure 6B). These results suggest that Cas-L and Tax possibly cooperate by protein–protein interaction mainly in the cytosol.

Exogenous Cas-L interferes with Tax-mediated transactivation of NF-κB

Tax is known as a potent transcriptional activator of host genes flanked by κB sequences as well as HTLV-I LTR. We examined the effect of Cas-L on Tax-associated κB- or TRE-dependent transactivation. As shown in Figure 7a, co-transfected Cas-L partially, but potently, inhibited Tax-mediated activation of an NF-κB-dependent transcription. This inhibitory activity was observed in all deletion mutants examined (Cas-LF, ΔSH3, ΔC, ΔSD), although the activity was weakest in Cas-LΔC, which is consistent with the co-immunoprecipitation assay (Figure 5d and e). On the other hand, Tax-mediated transcriptional enhancement of TRE-luciferase was not altered (Figure 7b). To assess the specificity of inhibition of κB-driven transcriptional activation, we next examined the effect of Cas-L on TNF-α (on 293T cells) or PMA (on Jurkat T cells)-stimulated activation of NF-κB. As shown in Figure 7c and d, expression of Cas-L or p130Cas did not affect NF-κB activation by these stimuli. These results strongly suggest that exogenous Cas-L specifically interferes with Tax-mediated activation of NF-κB.

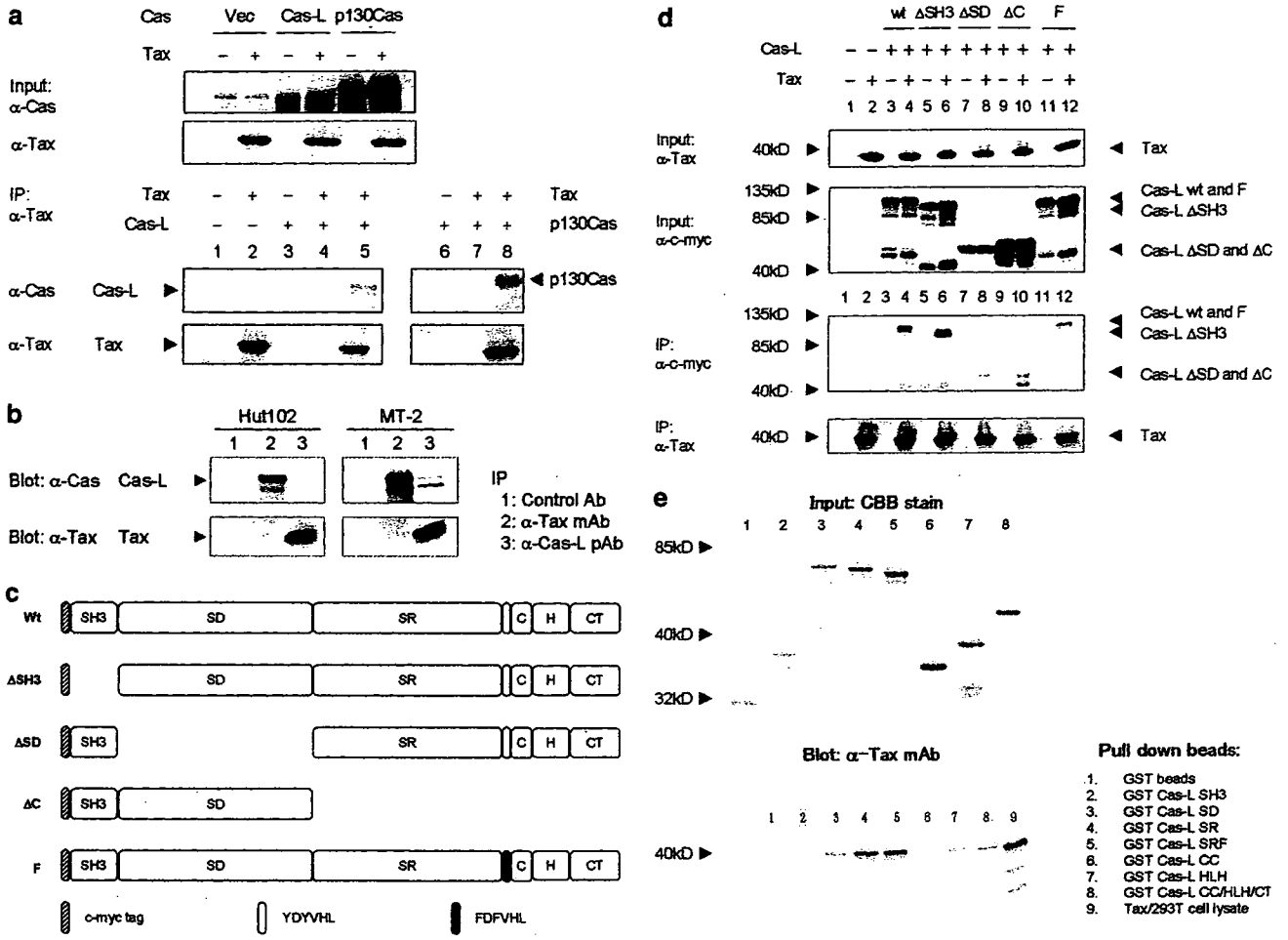

Figure 5 (a) Co-precipitation of Cas-L and p130Cas with Tax in 293T cells. 293T cells were transfected with pH2Rneo (−) or pH2Rneo-Tax (+), in the presence or absence of pSRalpha (Vec), pSRalpha Cas-L (Cas-L), or pSRalpha p130Cas (p130Cas). At 2 days after transfection, the cells were lysed with 1% Triton X-100 lysis buffer. *Input*: The lysates of 293T cells transfected with the indicated combination of plasmids were separated on SDS–PAGE, and subjected to immunoblotting with α-Cas mAb and α-Tax mAb. *IP*: Equal amounts of cellular lysates of 293T cells transfected with the indicated combination of plasmids were immunoprecipitated with isotype-matched control Ig (lanes 4, 7), anti-Tax mAb (lanes 1–3, 5, 6, 8). The precipitates were analysed by immunoblotting with anti-Cas mAb or anti-Tax mAb, respectively. (b) Co-precipitation of endogenous Cas-L and Tax in HTLV-I positive T cell lines. In toal, 1×10^7 of MT-2 cells and Hut102 cells were lysed with 1% Triton X-100 lysis buffer, then immunoprecipitated with the indicated antibodies. The immunoprecipitates were analysed by immunoblotting for anti-Cas mAb (the upper panel), and anti-Tax mAb (the lower panel). (c) Structure of Cas-L and its mutants. The secondary structure of Cas-L was graphically shown. The c-myc tag (MEQKLISEEDL) inserted 5′ prime to the second amino acid of Cas-L was visualized as dashed box. From 5′ prime, SH3: Src homology 3 domain, SD: substrate domain, SR: serine-rich region, C: Coiled-coil domain, H: helix–loop–helix domain, CT: c-terminal region. (d) Co-precipitation of Cas-L mutants with Tax in 293T cells. 293T cells were transfected with the indicated c-myc tagged Cas-L constructs (wt: pSRalpha c-myc Cas-L; ΔSH3: pSRalpha c-myc Cas-LΔSH3; ΔSD: pSRalpha c-myc Cas-LΔSD; ΔC: pSRalpha c-myc Cas-LΔC; F: pSRalpha c-myc Cas-LF; Vec: pSRalpha) either with pH2Rneo (−) or pH2RneoTAX (+). The top panel (*Input*): Equal amounts of cellular lysate from each transfected 293T cells were separated on SDS–PAGE and immunoblotted with anti-c-myc mAb. The middle panel (*α-c-myc*): Equal amounts of cellular lysate were immunoprecipitated with anti-Tax mAb, then analysed by immunoblotting with anti-c-myc mAb. The lower panel (*α-Tax*): The same membrane as the middle panel was reblotted with α-Tax mAb. (e) GST-pulldown assay with Cas-L mutants and Tax. The cellular lysates containing Tax were prepared by transfecting pH2Rneo-TAX by lipofectamine reagent. The lysates were incubated with recombinant GST-Cas-L domains immobilized on GSH-sepharose beads. The upper panel: Input of GST-fusion proteins were separated on SDS–PAGE, and visualized by CBB stain. Co-precipitated Tax proteins were separated on SDS–PAGE and subjected to immunoblotting with anti-Tax mAb (the lower panel). SRF: serine-rich region with FDFVHL, CC: coiled-coil domain, HLH: helix–loop–helix domain

Discussion

In the present study, we have shown that HTLV-I Tax may induce the expression and tyrosine phosphorylation of Cas-L. Using Jurkat T cells, we previously showed that gene transfer of Cas-L promoted cell motility on the ligands for $\beta 1$ integrins (i.e. FN and CS-1) in the presence or absence of anti-CD3 mAb stimulation (Ohashi *et al*., 1999). This enhancement was dependent on tyrosine phosphorylation of Cas-L, since the phosphorylation-deficient mutant of Cas-L (ΔSH3 and ΔSD) failed to enhance cell migration. Tax-induced JPX-9 cells clearly exhibited elevated level of tyrosine phosphorylation as well as elevated expression level of

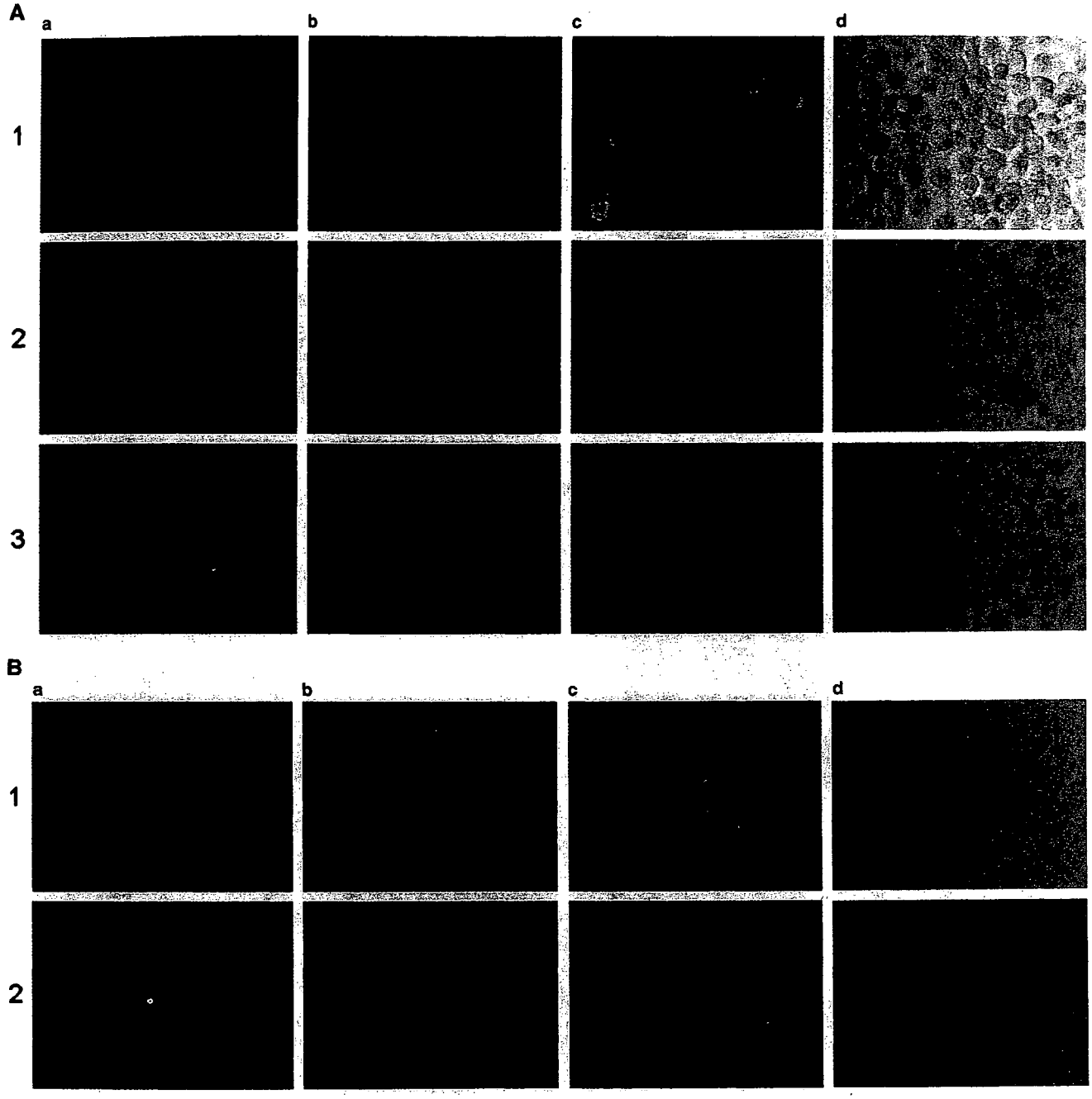

Figure 6 Co-localization of Cas-L with Tax in 293T cells. (**A**) 293T cells were transfected with pSRalpha c-myc Cas-L and pH2Rneo-Tax (row 1), pSRalpha c-myc Cas-L and pH2Rneo (row 2), pSRalpha and pH2Rneo-Tax (row 3) by lipofectamine on the glass coverslips. At 48 h after transfection, the cells were fixed and subjected to immunostaining. Subcellular localization of transfected proteins was analysed with confocal microscopy. Column a: Cy3-conjugated anti-c-myc mAbs; column b: anti-Tax mAb plus FITC-conjugated anti-mouse Ab; column c: merged results of the red (a) and green fluorescence (b) in the sequential mode; column d: phase contrast. (**B**) Hut-102 cells (row 1) and MT-2 cells (row 2) were cultured on the glass coverslips coated with FN at 5 μg/ml for overnight. The cells were fixed and subjected to immunostaining and confocal microscopic analysis. Column a: rabbit anti-CasL Ab plus FITC-conjugated anti-rabbit Ab; column b: anti-Tax mAb plus Texas Red-conjugated anti-mouse Ab; column c: merged results of the red (a) and green fluorescence (b) in the sequential mode; column d; phase contrast

Cas-L. These findings are of special interest since leukemic cells in ATL are notorious for extensive infiltrative activity toward organs and tissues, contributing to the unique clinical features of ATL (Uchiyama, 1996). A variety of molecules involved in cellular adhesion and migration are thought to play important roles in ATL pathophysiology, including MMP-9 (Mori *et al*., 2002), OX-40 (Imura *et al*., 1996), β1 integrins (especially VLA-4) (Ishikawa *et al*., 1993), and L-selectins (Ishikawa *et al*., 1993). Our current results

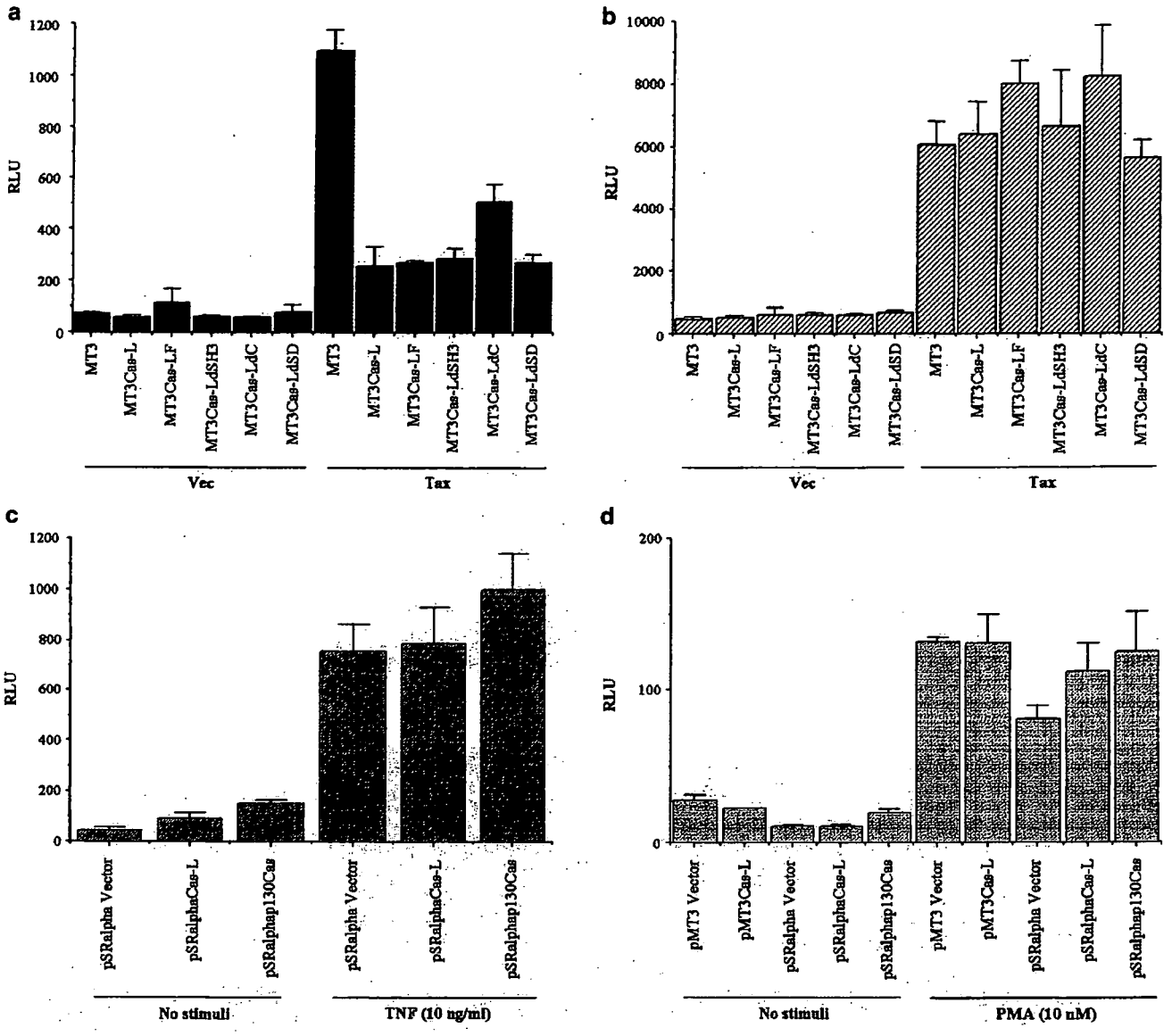

Figure 7 Effect of Cas-L expression on transactivation by Tax. (**a**, **b**) Jurkat-LT cells were transfected with NF-κB-Luc (**a**) or TRE-Luc (**b**), the indicated expression plasmids for wt (wild type) Cas-L, various Cas-L mutants, or pMT3 either with pH2Rneo (Vec) or pH2Rneo TAX by DMRIE-C. (**c**) 293T cells were transfected with NF-κB-Luc, the indicated plasmids for Cas-L, p130Cas, or pSRalpha by Lipofectamine. The cells were simultaneously stimulated with the indicated concentration of TNF-α or PMA. (**d**) Jurkat-LT cells were transfected with NF-κB-Luc, the indicated plasmids for Cas-L, p130Cas, or vector control (pSRalpha or pMT3) by DMRIE-C. The cells were simultaneously stimulated in the presence or absence of 10 ng/ml PMA. After 24 h, the lysates were subjected to luciferase assay (**a–d**)

imply that Cas-L may be one of targets for therapeutic intervention through modulation of its overexpression or tyrosine phosphorylation. Our results that the dominant-negative Cas-L mutants and FAK-CT inhibited Tax-mediated increase in cell motility indicating the involvement of Cas-L. However, it is still possible that some other Tax-inducible genes such as those described above might be involved in this phenomenon. The precise mechanism by which Cas-L was tyrosine-phosphorylated through the expression of Tax is an important question that remains to be elucidated.

It should be noted that the expression levels of Tax and Cas-L did not perfectly correlate in HTLV-I-transformed T cell lines and ATL-derived (MT-1 and H9) and patients samples from ATL. Indeed, in those clinical samples, the expression of Tax was hardly detected by immunoblotting (data not shown). This was consistent with the report that expression of Tax and viral mRNAs is tightly regulated *in vivo* by HTLV-I itself to escape from host defense mechanisms involving cytotoxic T lymphocytes reactive for Tax and env protein of HTLV-I (Yoshida, 1993). Therefore, the possibility exists that other undefined factors may contribute to the elevated expression of Cas-L *in vivo*.

In this study, we identified Tax as one of the Cas-L binding molecules. Others and we have shown that Cas

family proteins contain common structural motifs (Sakai *et al.*, 1994; Ishino *et al.*, 1995; Alexandropoulos and Baltimore, 1996; Law *et al.*, 1996; Minegishi *et al.*, 1996). It has been reported that some classes of Tax-binding proteins have coiled-coil domain, through which they associate with the same domain of Tax (Chun *et al.*, 2000). Unexpectedly, SR showed the strongest affinity for Tax, while SD and HLH only displayed some affinity. The significance of the interaction between Tax and these domains, especially in tyrosine phosphorylation of Cas-L, remains unclear. This important issue will be a main focus in future experiments.

To explore the effect of Tax-Cas-L interaction, we next analysed Tax-dependent transcriptional activation. Tax is a potent transactivator of numerous host genes besides being a cis-activator of the HTLV-I long terminal repeat. Among them, we compared the effect of Cas-L on NF-κB (Tax-dependent and Tax-independent) and TRE, and our results indicated that Cas-L may selectively interfere with Tax-mediated transactivation of NF-κB pathway. Due to methodological limitations involving the use of patient samples and HTLV-I infected cells that endogenously co-express Cas-L and Tax, we employed Jurkat T cells, which do not have detectable Tax expression and low level of Cas-L expression. Since the luciferase assay is a transient expression system, there is a possibility that Cas-L-mediated inhibition of NF-κB transactivation by Tax might reflect an artifact of overexpression. However, based on the findings that overexpression of Cas-L did not significantly alter other stimulatory signals that also induce NF-κB pathway (PMA, TNF-α), we believe that the observed phenomenon may still be biologically relevant.

Evaluating potential mechanisms by which Cas-L partially suppresses the Tax-mediated transactivation of NF-κB, we presented data suggesting that subcellular distribution of Tax was altered by the co-expression of Cas-L. Another possibility is that Cas-L may interact with other components of the NF-κB signaling pathway. Among them, IKK-α and IKK-β are known to possess HLH, through which they may associate with Cas family proteins. The possible interaction between Cas family members and IKK proteins and its impact on Tax-mediated transactivation remain to be solved in future.

In the clinical setting, our results that Cas-L might inhibit Tax-mediated transactivation of NF-κB appear to be contrary to the findings that Tax-mediated induction of Cas-L might be responsible for the invasive behavior of leukemic cells in ATL.

Our working hypothesis is that Cas-L may be a negative feedback regulator of the Tax/NF-κB system, potentially analogous to its role in the TGF-β/Smad system (Liu *et al.*, 2000). In the TGF-β/Smad system, Cas-L inhibits Smad3-mediated signaling by TGF-β by acting as a cytosolic sequestering protein for Smad3. On the other hand, it has been shown recently that TGF-β induces Cas-L (Zheng and McKeown-Longo, 2002).

Another possible interpretation is that induction of Cas-L by Tax might be a *double-edged sword*, since suppression of NF-κB-mediated transcription acts against leukemogenesis, whereas enhancement of cell motility contributes to the invasive nature of leukemic cells, which results in the complex clinical course of ATL as described above. Indeed, the clinical course of ATL is atypical in that the duration from viral infection to the clinical manifestation of leukemia often spans several decades.

In light of the fact that NF-κB is constitutively active in HTLV-I-transformed cells and ATL-derived T cell lines, which show also elevated Cas-L expression and Tax, it is possible that Cas-L-mediated suppression of transactivation by Tax might be overcome by unknown mechanisms during leukemogenesis. The discrepancy remains to be solved as a future question. Understanding the ontogeny of expression of Tax and Cas-L *in vivo* remains a difficult but critical point for evaluating the role of Cas-L in cellular transformation.

Together with previous results, the present findings suggest that Cas-L protein plays a crucial role in the pathophysiology of ATL. Additional investigations focusing on these new findings may lead to the eventual development of possible therapeutic applications of Cas-L gene products in HTLV-I-related diseases in the future.

Materials and methods

Antibodies and reagents

Anti-phosphotyrosine antibody (4G10) was purchased from Upstate Biotechnology, Inc. (Lake Placid, NY, USA). MAbs against FAK, Pyk2/CAKβ, p130Cas, and paxillin were obtained from Transduction Laboratories (Lexington, KY, USA). A rabbit polyclonal Ab (pAb) against Cas-L was described previously (Ohashi *et al.*, 1998). All chemicals were purchased from Sigma Chemical Co. (St Louis, MO, USA) unless otherwise stated. Mab against Tax (MI73) was kindly provided by Dr S. Yamaoka (Tokyo Medical and Dental University, Japan). Mab against c-myc tag (9E10) was produced from the hybridoma obtained from American Type Culture Collection (Manassas, VA, USA).

Plasmids

pCDSRα-CasL, pCDSRα-c-myc-Cas-L, pMT3-c-myc-Cas-L, pCDRSRα-p130Cas were described elsewhere (Tachibana *et al.*, 1997). The expression construct pCDSRα-c-myc-CasLΔSH3 lacks aa 1–60, pCDSRα-c-myc-CasLΔSD lacks aa 63–401, pCDSRα-c-myc-CasLΔC lacks aa 406–834 of Cas-L, respectively. In pCDSRα-c-myc-CasLF, Y629 and Y631 were mutated into F. pH2Rneo, pH2Rneo-wtTAX and pH2Rneo-40MTAX were kindly provided by Dr S Yamaoka (Tanaka *et al.*, 1990).

Cell lines, clinical samples from ATL patients and HTLV-I infected individuals

JPX-9 cells and JPX-M cells, kindly provided by Dr K Sugamura (Tohoku University School of Medicine), are derivatives of a human T cell line Jurkat, and have a stably integrated Tax gene under the control of a metallothionein

promoter (Nagata *et al.*, 1989). For the induction of Tax, the cells were cultured with 10 μM of $CdCl_2$.

Human peripheral blood mononuclear cells (PBMC) were isolated from heparinized blood of healthy volunteer donors, HTLV-I infected individuals, and patients with ATL by Ficoll-Hypaque density-gradient centrifugation, and washed with PBS. The diagnosis of ATL was based on clinical features, hematologic findings, and the presence of anti-HTLV-I antibodies in patient sera. All clinical samples were collected after informed consent was obtained.

Retroviral gene transfer

pMX-IRES-GFP and Plat-E were kindly provided by Dr T Kitamura (The Institute of Medical Science, The University of Tokyo, Japan) (Morita *et al.*, 2000). C-myc-tagged Cas-LΔSD, Cas-LΔC, and FAKCT (aa 709–1052) were subcloned into pMX-IRES-GFP. Plat-E cells were transfected using the Fugene6 reagent (Roche Applied Science, Indianapolis, IN, USA) with 1 μg of each retroviral vector. In total, 48 h post-transfection, the viral supernatant was used to infect PT-67 amphotropic packaging cell line (BD Biosciences Clontech, Palo Alto, CA, USA). After establishing PT-67 derived cell line stably producing each retrovirus, the supernatant was collected and used to infect JPX-9 cells at 32°C. After appropriate time period, GFP-positive cells were sorted by EPICS ELITE (Beckman Coulter, Inc., Tokyo, Japan).

Migration assays

Migration of JPX-9 cells was assayed using Transwell™ inserts with polycarbonate filter as described previously (Ohashi *et al.*, 1999). CS-1/GST fusion protein was described previously (Iwata *et al.*, 2002). The Transwell chambers containing 100 μl of 10^6 cells were inserted into wells filled with 600 μl of 0.6% BSA RPMI1640. After incubation at 37°C, the filters were stained with May-Giemsa solutions. The number of migrated cells to the lower side of the filters was counted microscopically in five high-power fields per insert at $\times$400 magnification. Each experiment was performed in triplicate wells.

Immunoprecipitation and immunoblotting

For immunoprecipitation, cells were lysed in 1% Triton X-100 lysis buffer (Iwata *et al.*, 2002). Briefly, cellular lysates were incubated with appropriate first Ab at 4°C overnight, and then with protein A sepharose beads for 4 h. The beads were washed with 1% Triton X-100 lysis buffer, and heated to 95°C in the SDS–PAGE loading buffer. The supernatants were loaded onto 8% SDS–PAGE gels, electro-transferred onto PVDF membranes. After blocking, membranes were incubated with the primary Ab, then washed and incubated with HRP-conjugated anti-mouse IgG Ab. The membranes were developed by the enhanced chemiluminescence (ECL) system (Amersham Biosciences, Piscataway, NJ, USA).

Yeast two-hybrid screening

The two-hybrid analysis was carried out essentially as described previously (Durfee *et al.*, 1993), using pACTII (for GAL4 activator domain) and pBTM116 (for LexA DNA-binding domain). cDNA encoding full-length Cas-L was cloned into pBTM116. The resulting plasmid, pBTM116-Cas-L, was used as bait in a two-hybrid screen of a cDNA library of human HTLV-I infected T cell line (SLB-I) (BD Biosciences Clontech) in *S. cerevisiae* L40. Positive yeast clones were selected for histidine prototrophy and expression of β-galactosidase. Plasmids containing cDNA clones were rescued from yeast and characterized by DNA sequencing.

Immunofluorescence and confocal microscopy

Transfected cells cultured on the glass coverslips were fixed by immersion in 3.7% PBS-paraformaldehyde solution for 10 min, and permeabilized with PBS-0.1% Triton X-100 for 10 min. After blocking with 1% BSA-PBS, slips were incubated with the primary antibodies for 1 h, then washed and incubated with Cy3-, Texas Red- or FITC-conjugated appropriate second antibodies for one additional hour. After washing, slips were mounted and observed using an argon–krypton laser confocal microscope (FV500, OLYMPUS, Tokyo, Japan).

GST-pull down assay

The coding regions for Cas-L SH3 (aa 1–77), SD (substrate domain) (aa 62–359), SR (serine-rich region) (aa 350–639), CC (coiled-coil domain) (aa 635–700), HLH (helix–loop–helix domain) (aa 678–775), or CC/HLH/CT (c-terminal region) (aa 635–834) were PCR-amplified and subcloned into the pGEX-2T vector. GST-SRF contains aa 350–639 of Cas-L with Y629F and Y631F mutation. GST or GST-Cas-L domains expressed in *E. coli* were purified by adsorption to glutathione sepharose 4B beads. Those proteins preimmobilized on 5 μl of 50% slurry of the brads were incubated with cellular lysates from Tax-transfected 293T cells (50 μg total protein) for 4 h at 4°C. Following incubation, the bound matrices were washed with 1% Triton X-100 lysis buffer, and then subjected to 12% SDS–PAGE and immunoblotting, as described.

Transfection and luciferase assay

Transfection and Luciferase reporter assay were performed as described previously with some modification (Iwata *et al.*, 2002). Briefly, Dual-Luciferase™ Reporter Assay System (Promega, Madison, WI, USA) was used to measure Luciferase activity expressed by the experimental plasmids pNF-κB-Luc (Stratagene, La Jolla, CA, USA) and pHTLV-Luc (TRE-Luc). pNF-κB-Luc has 5 $\times$ tandem repeat of κB enhancer element and pHTLV-Luc contains 1–650 bp of HTLV-I LTR (U3-R part of U5). For the internal control, pRL-TK was employed. The enzyme activities of firefly luciferase and Renilla luciferase were measured by luminometer (Model TD-20/20, Turner Design, Inc., Sunnyvale, CA, USA).

Acknowledgements

We appreciate Yoshiyuki Ohashi, Rikako Miyake-Nishijima, Seiji Kobayashi, Kei Ohnuma, Masahiko Uchiyama, Rika Ouchida, and Noriaki Shimizu for help in some experiments. We greatly acknowledge Shoji Yamaoka for critical reading of the manuscript and invaluable discussion. This work was supported by grants-in-aid from the Ministry of Education, Science, and Culture and Ministry of Health, Labor and Welfare, of Japan.

References

Albrecht H, Shakhov AN and Jongeneel CV. (1992). *J. Virol.*, **66**, 6191–6193.

Alexandropoulos K and Baltimore D. (1996). *Genes Dev.*, **10**, 1341–1355.

Chun AC, Zhou Y, Wong CM, Kung HF, Jeang KT and Jin DY. (2000). *AIDS Res. Hum. Retroviruses*, **16**, 1689–1694.
Cross SL, Feinberg MB, Wolf JB, Holbrook NJ, Wong-Staal F and Leonard WJ. (1987). *Cell*, **49**, 47–56.
Durfee T, Becherer K, Chen PL, Yeh SH, Yang Y, Kilburn AE, Lee WH and Elledge SJ. (1993). *Genes Dev.*, **7**, 555–569.
Franchini G. (1995). *Blood*, **86**, 3619–3639.
Fujii M, Niki T, Mori T, Matsuda T, Matsui M, Nomura N and Seiki M. (1991). *Oncogene*, **6**, 1023–1029.
Fujii M, Sassone-Corsi P and Verma IM. (1988). *Proc. Natl. Acad. Sci. USA*, **85**, 8526–8530.
Harhaj EW and Sun SC. (1999). *J. Biol. Chem.*, **274**, 22911–22914.
Hemler ME. (1990). *Annu. Rev. Immunol.*, **8**, 365–400.
Hynes RO. (1992). *Cell*, **69**, 11–25.
Imura A, Hori T, Imada K, Ishikawa T, Tanaka Y, Maeda M, Imamura S and Uchiyama T. (1996). *J. Exp. Med.*, **183**, 2185–2195.
Inoue J, Seiki M, Taniguchi T, Tsuru S and Yoshida M. (1986). *EMBO J.*, **5**, 2883–2888.
Ishikawa T, Imura A, Tanaka K, Shirane H, Okuma M and Uchiyama T. (1993). *Blood*, **82**, 1590–1598.
Ishino M, Ohba T, Sasaki H and Sasaki T. (1995). *Oncogene*, **11**, 2331–2338.
Iwata S, Kobayashi H, Miyake-Nishijima R, Sasaki T, Souta-Kuribara A, Nori M, Hosono O, Kawasaki H, Tanaka H and Morimoto C. (2002). *Eur. J. Immunol.*, **32**, 1328–1337.
Juliano RL and Haskill S. (1993). *J. Cell Biol.*, **120**, 577–585.
Kim SJ, Kehrl JH, Burton J, Tendler CL, Jeang KT, Danielpour D, Thevenin C, Kim KY, Sporn MB and Roberts AB. (1990). *J. Exp. Med.*, **172**, 121–129.
Law SF, Estojak J, Wang B, Mysliwiec T, Kruh G and Golemis EA. (1996). *Mol. Cell Biol.*, **16**, 3327–3337.
Liu X, Elia AE, Law SF, Golemis EA, Farley J and Wang T. (2000). *EMBO J.*, **19**, 6759–6769.
Maruyama M, Shibuya H, Harada H, Hatakeyama M, Seiki M, Fujita T, Inoue J, Yoshida M and Taniguchi T. (1987). *Cell*, **48**, 343–350.
Matsuyama T, Yamada A, Kay J, Yamada KM, Akiyama SK, Schlossman SF and Morimoto C. (1989). *J. Exp. Med.*, **170**, 1133–1148.
Minegishi M, Tachibana K, Sato T, Iwata S, Nojima Y and Morimoto C. (1996). *J. Exp. Med.*, **184**, 1365–1375.
Miura S, Ohtani K, Numata N, Niki M, Ohbo K, Ina Y, Gojobori T, Tanaka Y, Tozawa H and Nakamura M. (1991). *Mol. Cell. Biol.*, **11**, 1313–1325.
Miyake-Nishijima R, Iwata S, Saijo S, Kobayashi H, Kobayashi S, Souta-Kuribara A, Hosono O, Kawasaki H, Tanaka H, Ikeda E, Okada Y, Iwakura Y and Morimoto C. (2003). *Arthritis Rheum.*, **48**, 1890–1900.
Mori N, Mukaida N, Ballard DW, Matsushima K and Yamamoto N. (1998). *Cancer Res.*, **58**, 3993–4000.
Mori N, Sato H, Hayashibara T, Senba M, Hayashi T, Yamada Y, Kamihira S, Ikeda S, Yamasaki Y, Morikawa S, Tomonaga M, Geleziunas R and Yamamoto N. (2002). *Blood*, **99**, 1341–1349.
Morita S, Kojima T and Kitamura T. (2000). *Gene Ther.*, **7**, 1063–1066.
Nagata K, Ohtani K, Nakamura M and Sugamura K. (1989). *J. Virol.*, **63**, 3220–3226.
Nojima Y, Humphries MJ, Mould AP, Komoriya A, Yamada KM, Schlossman SF and Morimoto C. (1990). *J. Exp. Med.*, **172**, 1185–1192.
Nojima Y, Rothstein DM, Sugita K, Schlossman SF and Morimoto C. (1992). *J. Exp. Med.*, **175**, 1045–1053.
Ohashi Y, Iwata S, Kamiguchi K and Morimoto C. (1999). *J. Immunol.*, **163**, 3727–3734.
Ohashi Y, Tachibana K, Kamiguchi K, Fujita H and Morimoto C. (1998). *J. Biol. Chem.*, **273**, 6446–6451.
Ruoslahti E and Reed JC. (1994). *Cell*, **77**, 477–478.
Sakai R, Iwamatsu A, Hirano N, Ogawa S, Tanaka T, Mano H, Yazaki Y and Hirai H. (1994). *EMBO J.*, **13**, 3748–3756.
Sato T, Tachibana K, Nojima Y, D'Avirro N and Morimoto C. (1995). *J. Immunol.*, **155**, 2938–2947.
Sodroski JG, Rosen CA and Haseltine WA. (1984). *Science*, **225**, 381–385.
Tachibana K, Sato T, D'Avirro N and Morimoto C. (1995). *J. Exp. Med.*, **182**, 1089–1099.
Tachibana K, Urano T, Fujita H, Ohashi Y, Kamiguchi K, Iwata S, Hirai H and Morimoto C. (1997). *J. Biol. Chem.*, **272**, 29083–29090.
Tanaka A, Takahashi C, Yamaoka S, Nosaka T, Maki M and Hatanaka M. (1990). *Proc. Natl. Acad. Sci. USA*, **87**, 1071–1075.
Uchiyama T, Yodoi J, Sagawa K, Takatsuki K and Uchino H. (1977). *Blood*, **50**, 481–492.
Uchiyama T. (1996). *J. Clin. Immunol.*, **16**, 305–314.
Yamashita I, Katamine S, Moriuchi R, Nakamura Y, Miyamoto T, Eguchi K and Nagataki S. (1994). *Blood*, **84**, 1573–1578.
Yodoi J and Uchiyama T. (1986). *Immunol. Rev.*, **92**, 135–156.
Yoshida M. (1993). *Trends Microbiol.*, **1**, 131–135.
Yoshimura T, Fujisawa J and Yoshida M. (1990). *EMBO J.*, **9**, 2537–2542.
Zheng M and McKeown-Longo PJ. (2002). *J. Biol. Chem.*, **277**, 39599–39608.

Regulation of p38 Phosphorylation and Topoisomerase IIα Expression in the B-Cell Lymphoma Line Jiyoye by CD26/Dipeptidyl Peptidase IV Is Associated with Enhanced *In vitro* and *In vivo* Sensitivity to Doxorubicin

Toshiko Yamochi,[1] Tadanori Yamochi,[1] Ugur Aytac,[1] Tsutomu Sato,[1] Kazuya Sato,[1] Kei Ohnuma,[2] Kathryn S. McKee,[1] Chikao Morimoto,[1,2] and Nam H. Dang[1]

[1]Department of Lymphoma/Myeloma, University of Texas M.D. Anderson Cancer Center, Houston, Texas and [2]Department of Clinical Immunology, Institute of Medical Science, University of Tokyo, Tokyo, Japan

Abstract

CD26 is a M_r 110,000 surface-bound glycoprotein with diverse functional properties, including having a key role in normal T-cell physiology and the development of certain cancers. In this article, we show that surface expression of CD26, especially its intrinsic dipeptidyl peptidase IV (DPPIV) enzyme activity, results in enhanced topoisomerase IIα level in the B-cell line Jiyoye and subsequent *in vitro* sensitivity to doxorubicin-induced apoptosis. In addition, we show that expression of CD26/DPPIV is associated with increased phosphorylation of p38 and its upstream regulators mitogen-activated protein kinase kinase 3/6 and apoptosis signal-regulating kinase 1 and that p38 signaling pathway plays a role in the regulation of topoisomerase IIα expression. Besides demonstrating that CD26 effect on topoisomerase IIα and doxorubicin sensitivity is applicable to cell lines of both B-cell and T-cell lineages, the potential clinical implication of our work lies with the fact that we now show for the first time that our *in vitro* results can be extended to a severe combined immunodeficient mouse model. Our findings that CD26 expression can be an *in vivo* marker of tumor sensitivity to doxorubicin treatment may lead to future treatment strategies targeting CD26/DPPIV for selected human cancers in the clinical setting. Our article thus characterizes the biochemical linkage among CD26, p38, and topoisomerase IIα while providing evidence that CD26-associated topoisomerase IIα expression results in greater *in vitro* and *in vivo* tumor sensitivity to the antineoplastic agent doxorubicin. (Cancer Res 2005; 65(5): 1973-83)

Introduction

CD26 is a M_r 110,000 type II cell surface glycoprotein with diverse functional properties, which is widely expressed on various tissues, including lymphocytes, with its extracellular domain encoding a membrane-associated dipeptidyl peptidase IV (DPPIV) activity that cleaves selected biological factors to alter their functions (1). It plays an important role in T-cell biology through its physical and functional association with molecules involved in T-cell signal transduction processes (1–6). Recent findings suggest that CD26/DPPIV has a role in the development of certain neoplasms, being overexpressed in certain aggressive T-cell malignancies (7, 8), B-chronic lymphocytic leukemia (9), and thyroid carcinoma (10). On the other hand, loss or decreased surface expression of CD26/DPPIV is found in prostate cancer (11), colorectal carcinoma (12), and melanomas (13). Meanwhile, investigators have shown that DPPIV expression in melanoma and non–small cell lung carcinoma leads to inhibition of tumorigenicity, whereas DPPIV expression in ovarian carcinoma cells reduces i.p. dissemination of carcinoma cells and prolongs survival time (14–16). Topoisomerase IIα is an intracellular protein with a key role in proliferation and is a target for various antineoplastic agents (17). We found recently that CD26/DPPIV expression on the T-cell line Jurkat is associated with increased topoisomerase IIα level, leading to a concomitant enhancement in *in vitro* sensitivity to topoisomerase II inhibitors (18–20).

The family of mitogen-activated protein kinases (MAPK) plays a very important role in the signal pathways of cell proliferation, differentiation, survival, and apoptosis (21). Three major molecules belong to this family: extracellular signal-regulated kinase (ERK) 1/2 (p44/p42), c-Jun NH_2-terminal kinase (JNK/stress-activated protein kinase), and p38 MAPKs. In general, the ERK pathway mediates primarily cell growth and survival signals and promotes induction of cell differentiation under certain circumstances. On the other hand, both JNK and p38 pathways, which comprise the stress-activated protein kinase family, generally mediate proapoptotic, growth inhibitory signals and proinflammatory responses. However, p38 also induces antiapoptotic, proliferative, and cell survival signals under certain conditions (22, 23). Of note is the fact that certain antineoplastic agents, such as doxorubicin and cisplatin, induce p38-mediated apoptosis (23, 24). CD26/DPPIV is also associated with p38 signaling in certain instances. Inhibition of DPPIV enzyme activity resulted in p38 activation, leading subsequently to transforming growth factor-β1 expression and secretion (25). Meanwhile, ERK was phosphorylated and activated in CD26 Jurkat transfectant following treatment with anti-CD26 antibody (26).

Extending our previous findings in this study, we use the Burkitt B-cell lymphoma line Jiyoye to characterize the effect of CD26 expression on topoisomerase IIα and p38. We show that CD26 expression on CD26 Jiyoye transfectants is associated with enhanced topoisomerase IIα level and increased sensitivity to the antineoplastic agent doxorubicin. We also show that CD26 expression results in increased p38 phosphorylation, associated with increased phosphorylation of the upstream regulators MAPK

Requests for reprints: Nam H. Dang, Department of Lymphoma/Myeloma, University of Texas M.D. Anderson Cancer Center, 1515 Holcombe Boulevard, Box 429, Houston, TX 77030. Phone: 713-792-2860; Fax: 713-794-5656; E-mail: nhdang@mail.mdanderson.org.

kinase (MKK) 3/6 and apoptosis signal-regulating kinase 1 (ASK1). Inhibition of p38 phosphorylation decreases topoisomerase IIα expression, suggesting a role for p38 in the regulation of topoisomerase IIα. Finally, studies using a severe combined immunodeficient (SCID) mouse xenograft model with CD26 Jiyoye transfectants show that CD26 expression is associated with enhanced survival following treatment with low doses of doxorubicin. Our data thus characterize the biochemical linkage among CD26, p38, and topoisomerase IIα while suggesting a potential role for CD26 in the clinical setting in the treatment of selected malignancies.

Materials and Methods

Animals, Cells, and Reagents. Human Burkitt B-cell lymphoma cell line Jiyoye and human anaplastic large T-cell lymphoma cell line Karpas-299 were obtained from American Type Culture Collection (Rockville, MD). Jiyoye cells were maintained in culture medium, which consisted of RPMI 1640 supplemented with 20% FCS, 100 units/mL penicillin, and 100 μg/mL streptomycin at 37°C and 5% CO_2. Karpas-299 cells were maintained in RPMI 1640 supplemented with 10% FCS and penicillin-streptomycin at 37°C and 5% CO_2. Female CB-17 SCID mice were obtained from Taconic Farms, Inc. (Germantown, NY) at 3 weeks of age and were housed in microisolator cages, and all food, water and bedding were autoclaved before use. Annexin V-FITC, anti-poly(ADP-ribose) polymerase, phycoerythrin-conjugated anti-CD19, and phycoerythrin-conjugated anti-CD8 were from BD PharMingen (San Diego, CA); FITC-conjugated anti-CD26 was from Caltag (Burlingame, CA); anti-actin was from Sigma Chemical Co. (St. Louis, MO); anti-topoisomerase IIα was from Roche (Indianapolis, IN); antibodies against p38, phospho-p38, ERK1/2 (p44/p42 MAPK), phospho-ERK1/2, JNK, phospho-JNK, MKK3, phospho-MKK3/MKK6, ASK1, and phospho-ASK1 (Ser^{83} and Ser^{967}) were purchased from Cell Signaling Technology, Inc. (Beverly, MA). The p38 inhibitor SKF86002 was from Calbiochem (La Jolla, CA). Substrate for DPPIV, Gly-Pro-*p*-nitroanilide-tosylate, was purchased from WAKO (Osaka, Japan). Doxorubicin was purchased from Calbiochem and was dissolved in sterile PBS. All oligonucleotides were synthesized with Invitrogen (Carlsbad, CA).

Establishment of CD26 Transfectants. The CD26 cDNA insert was prepared from the plasmid pSRa-26 as described previously (27). 5′ Flanking region of CD26 (28) was extended and amplified by the PCR used with primers Ad1 (CCCGGGTCTGCCTGCGCTCCTTCTCTGAACGCTCACTTCCGAGGAGACGCCGACGATGAAGACACC) and R3 (GCGCGGTACCCTAAGGTAAAGAGAAACATTG). Through site-directed gene mutagenesis method (29), mutant CD26 containing an alanine at the putative catalytic Ser^{630} was prepared with primers Ad1, R3, and SA (AATTTGGGGCTGGGCATATGGAGGGTACGT), resulting in a mutant CD26 positive-DPPIV negative (S630A; ref. 30). After the sequences were confirmed, CD26 or CD26S630A fragment was inserted into retroviral vector pLNCX2 containing a neomycin-selection marker, which was obtained from Clontech Laboratories, Inc. (Palo Alto, CA). To generate the recombinant, the dualtropic retroviral packaging cell line GP2-293 was transfected by Plus Reagent (Invitrogen) and LipofectAMINE reagent (Invitrogen) with p10A1 (Clontech Laboratories) and recombinant vectors as per manufacturer's protocol. Seventy-two hours after transfection, the supernatants containing retrovirus expressing CD26 or CD26S630A were collected, filtered through a 0.45 μm syringe filter, and used to transduce target cells. To transduce Jiyoye cells, viral supernatant was added with polybrene (final concentration 8 μg/mL, Sigma Chemical) and the cells were incubated at 37°C for 24 hours; then, the medium was replaced with fresh medium containing G418 (1.5 mg/mL, Life Technologies, Grand Island, NY).

Small Interfering RNA Studies. To design target-specific small interfering RNA (siRNA) duplexes, we selected sequences of the type AA (N19; N, any nucleotide) from the open reading frame of CD26 mRNA (accession no. NM 001935) by Dharmacon siDESIGN Center (Lafayette, CO). We selected the target sequence from 1,768 to 1,786 downstream of the start codon of CD26 mRNA. Inserted siRNA oligonucleotide of pSilencerRetroQ vector (Clontech Laboratories) was designed according to manufacturer's protocol. The inserted sequence was as follows: sense GATCCGATCATGCATGCAATCAACTTCAAGAGAGTTGATTGCATGCATGATCTTTTTTGGAAG [sense siRNA (CD26-siRNA)] and antisense AATTCTTCCAAAAAAGATCATGCATGCAATCAACTCTCTTGAAGTTGATTGCATGCATGATCG. Moreover, missense siRNA [mis-siRNA (mis-CD26-siRNA)] at 3 nt was prepared to examine nonspecific effects of siRNA duplexes. Inserted sequence was as follows: sense GATCCGATCTTGCAAGCAAACAACTTCAAGAGAGTTGTTTGCTTGCAAGATCTTTTTTGGAAG and antisense AATTCTTCCAAAAAAGATCTTGCAAGCAAACAACTCTCTTGAAGTTGTTTGCTTGCAAGATCG. These sense and antisense primers were hybridized and then inserted into pSilencerRetroQ vector. After all sequences were confirmed, CD26-siRNA retrovirus was produced by the same method as above, and Karpas-299 cells were transduced and selected with puromycin (0.4 μg/mL, Clontech Laboratories).

3-(4,5-Dimethylthiazol-2-yl)-2,5-Diphenyltetrazolium Bromide Assay. Cell growth assay was done as described previously (31). Cells were incubated in 96-well plates in the presence of culture medium alone or culture medium with doxorubicin at the indicated concentrations for a total volume of 100 μL (50,000 cells per well). After 72 hours of incubation at 37°C, 3-(4,5-dimethylthiazol-2-yl)-2,5-diphenyltetrazolium bromide (25 μL) was added to the wells at a final concentration of 1 mg/mL. The 96-well plates were then incubated for 2 hours at 37°C followed by the addition of 100 μL extraction buffer. After overnight incubation at 37°C, absorbance measurements at 570 nm were done, with SE of the triplicate well being <15%.

Cytotoxicity index was calculated as follows:

$$\text{Cytotoxicity index (\% of control)} = 1 - \frac{A_{570\text{ nm}} \text{ of treated cells}}{A_{570\text{ nm}} \text{ of control cells}} \times 100\%$$

Immunofluorescence. All procedures were carried out at 4°C and flow cytometric analyses were done (FACScan, Becton Dickinson, San Jose, CA) as described previously (32). Cells were stained with FITC-conjugated anti-CD26 antibody and washed twice with PBS and then with goat anti-mouse IgG FITC (Coulter, Fullerton, CA). Cells were then washed twice with PBS before flow cytometric analysis. Negative control samples were stained with second antibody alone.

Annexin V/Propidium Iodide Assays. Exposure of phosphatidylserine residues was quantified by surface Annexin V staining as described previously (33). Briefly, cells were washed in binding buffer [10 mmol/L HEPES (pH 7.4), 2.5 mmol/L $CaCl_2$, 140 mmol/L NaCl], resuspended in 100 μL, and incubated with 0.5 μL/mL Annexin V-FITC and 2.5 μg/mL propidium iodide (PI) for 15 minutes in the dark. Cells were then washed again and resuspended in 400 μL binding buffer; then, flow cytometric analysis was done. A total of 10,000 cells were acquired per sample and data were analyzed using CellQuest software (BD PharMingen). Cells in early stages of apoptosis were Annexin V positive, whereas cells that were Annexin V and PI positive were in late stages of apoptosis (34).

SDS-PAGE and Immunoblotting. After incubation at 37°C in culture medium, Jiyoye-vector control, Jiyoye-wild-type (wt) CD26 transfectant, and Jiyoye-SACD26 transfectant were harvested, washed with PBS, and lysed in lysis buffer consisting of 1% NP40, 0.5% deoxycholate, 0.1% SDS, 1 mmol/L phenylmethylsulfonyl fluoride, 1 mmol/L benzamidine, 10 μg/mL aprotinin, 50 μg/mL leupeptin, 10 μg/mL soybean trypsin inhibitor, and 1 μg/mL pepstatin. After incubating on ice for 5 minutes, nuclei were removed by centrifugation and supernatants were collected as whole cell lysates. Sample buffer (4×) consisting of 20% glycerol, 4.6% SDS, 0.5 mol/L Tris (pH 6.8), 4% β-mercaptoethanol, and 0.2% bromophenol blue was added to the appropriate aliquots of supernatants. After boiling, protein samples were submitted to SDS-PAGE analysis on appropriate gel under standard conditions using mini-Protein II system (Bio-Rad, Richmond, CA). For each experiment, each lane was loaded with equal amount of protein. For immunoblotting, the proteins were transferred onto nitrocellulose (Immobilon-P, Millipore, Billerica, MA).

After blocking for 1 hour at room temperature or overnight at 4°C in blocking solution consisting of 5% bovine serum albumin or 5% dry milk in 0.1% Tween 20-TBS, membranes were blotted with the appropriate primary antibodies diluted in blocking solution for 1 hour at room temperature or overnight at 4°C. Membranes were then washed with Tween 20-TBS, and appropriate secondary antibodies diluted in Tween 20-TBS were then applied for 1 hour at room temperature. Secondary antibody was goat anti-rabbit or goat anti-mouse horseradish peroxidase conjugates (DAKO, Kyoto, Japan). Membranes were then washed with Tween 20-TBS, and proteins were detected using an enhanced chemiluminescence system according to the manufacturer's instructions (Pierce, Rockford, IL). Membranes were exposed to Hyperfilm (Amersham Pharmacia Biotech, Piscataway, NJ).

DPPIV Enzyme Activity Assay. As described previously (16), DPPIV enzyme activity was measured spectrophotometrically using Gly-Pro-*p*-nitroanilide-tosylate, a substrate for DPPIV. A 1× PBS-washed whole cell suspension was prepared, and 5×10^5 cells were resuspended in 200 μL PBS into 96-well plate; then, Gly-Pro-*p*-nitroanilide-tosylate was added at a final concentration of 0.24 mmol/L. The absorption was measured at 405 nm using microplate spectrophotometer (BIO-TEK Instruments, Inc., Winooski, VE) twice just before the addition of the substrate and after 60-minute incubation at 37°C. DPPIV enzyme activity was calculated from the increase of absorption between 0 and 60 minutes.

Preparation of Nuclear Extracts for Detection of Topoisomerase IIα Protein Level. For detection of topoisomerase IIα by immunoblotting, isolation of nuclear fractions from Jiyoye-CD26 transfectants was prepared as follows. In brief, 10×10^6 cells were harvested and allowed to swell for 15 minutes on ice in cytoplasmic extraction buffer (10 mmol/L HEPES, 10 mmol/L KCl, 0.1 mmol/L EDTA, 0.1 mmol/L EGTA, 1 mmol/L DTT, 1 mmol/L phenylmethylsulfonyl fluoride, 2 μg/mL leupeptin, 2 μg/mL aprotinin, and 0.5 mg/mL benzamidine). Then, NP40 (final concentration 0.3%) was added to the cell suspension and vortexed for 10 seconds. After 2 minutes of centrifugation at 16,000 × *g*, the supernatant was removed. The pellet was then incubated with nuclear extraction buffer (20 mmol/L HEPES, 400 mmol/L KCl, 1 mmol/L EDTA, 1 mmol/L EGTA, 1 mmol/L DTT, 0.5 mmol/L phenylmethylsulfonyl fluoride, 2 μg/mL leupeptin, 2 μg/mL aprotinin, and 0.5 mg/mL benzamidine) for 30 minutes on ice with intermittent vortexing. The suspension was centrifuged at 16,000 × *g* for 5 minutes, and the supernatant was saved as the nuclear extract. SDS-PAGE and immunoblotting were then done on the nuclear extracts. Each lane was equally loaded with 10 μg protein.

***In vivo* Experiments.** All mice were pretreated by i.p. route with 0.2 mL anti-asialo-GM1 polyclonal antisera 25% (v/v, WAKO) 1 day before tumor transplant to eliminate host natural killer cell activity and facilitate tumor engraftment (35). On day 0, 7×10^6 Jiyoye-wtCD26 transfectant cells or Jiyoye-vector control cells were then inoculated by i.p. injection. Following tumor cell inoculation, SCID mice then received saline or doxorubicin in saline by i.p. injection at 0.5 mg/kg on days 1 and 15. Tumor bearing mice were monitored for tumor development and progression, and moribund mice were euthanized, with necropsies being done for evidence of tumors. In addition, mice with visible or palpable tumors measuring 15 mm at its smallest dimension were euthanized, with necropsies done to minimize suffering to the mice.

Results

Expression of CD26/DPPIV and Topoisomerase IIα in Jiyoye-CD26 Transfectants. Following transfection of the human Burkitt B-cell lymphoma cell line Jiyoye with the retroviral vector pLNCX2 as described in Materials and Methods, CD26/DPPIV status is evaluated. Parental Jiyoye cells and pLNCX2-only Jiyoye transfectants (Jerome-vector control) do not express detectable amount of CD26 as determined by cell surface staining. Meanwhile, Jiyoye-wtCD26 transfectants have high level of CD26 surface expression, and Jiyoye-S630A (SACD26) transfectants express the catalytically inactive variant of CD26 (Fig. 1*A*). On the other hand, only the Jiyoye-wtCD26 transfectants express DPPIV enzyme activity, with Jiyoye-vector control and Jiyoye-SACD26 transfectants having no detectable DPPIV activity (Fig. 1*B*). Consistent with our previous findings that CD26 expression is associated with increased topoisomerase IIα level in CD26 transfectants of the T-cell leukemia line Jurkat (19, 20), Jiyoye-wtCD26 transfectants also express higher level of topoisomerase IIα than Jiyoye-vector control or Jiyoye-SACD26 transfectants (Fig. 1*C*). By demonstrating that CD26 expression, particularly its DPPIV enzyme activity, is associated with enhanced topoisomerase IIα expression in the B-cell line Jiyoye, our findings indicate that a relationship between these key proteins is potentially found in a wide variety of tumor types. Furthermore, our data suggest a potential role for CD26/DPPIV in the treatment of malignancies of both B-cell and T-cell lineages.

Enhancement of Doxorubicin-Mediated Apoptosis in Jiyoye-CD26 Transfectants. To elucidate the potential consequence of the CD26-topoisomerase IIα association, we investigated the effect of CD26/DPPIV surface expression on doxorubicin sensitivity of Jiyoye-CD26 stable transfectants. 3-(4,5-Dimethylthiazol-2-yl)-2,5-diphenyltetrazolium bromide uptake assays show that Jiyoye-wtCD26 transfectants display significantly increased sensitivity to doxorubicin compared with Jiyoye-vector control. In addition, Jiyoye-SACD26 transfectant, with CD26 mutated at the DPPIV catalytic site (S630A), is less sensitive to doxorubicin than Jiyoye-wtCD26 transfectants, consistent with the key role played by the DPPIV enzyme activity in increasing topoisomerase IIα level and subsequent drug sensitivity (Fig. 2*A*). Meanwhile, Annexin V-PI assays show greater doxorubicin-induced apoptosis for Jiyoye-wtCD26 transfectants than Jiyoye-vector control cells or Jiyoye-SACD26 transfectants (Fig. 2*B*). Furthermore, Western blot analyses show that Jiyoye-wtCD26 transfectants exhibit greater poly(ADP-ribose) polymerase cleavage with doxorubicin treatment than Jiyoye-vector cells (Fig. 2*C*) Taken together, these data show that surface expression of CD26/DPPIV on the B-cell lymphoma line Jiyoye directly enhances cellular sensitivity to doxorubicin and drug-induced apoptosis.

Effect of CD26/DPPIV Surface Expression on the p38 Signaling Pathway. Because CD26 signaling involves MAPK in certain experimental conditions (25, 26), we evaluated the status of p38, ERK, and JNK in Jiyoye-CD26 transfectants. Figure 3 shows that Jiyoye-wtCD26 transfectants exhibit greater phosphorylation of p38 compared with Jiyoye-vector or Jiyoye-SACD26 transfectant in the absence of any extrinsic stimulation. In contrast to p38, there is no difference in the phosphorylation status of ERK and JNK among the cells incubated in culture medium, confirming that p38 is selectively phosphorylated in the presence of CD26, particularly its DPPIV enzyme activity.

To further confirm our findings with the Jiyoye-CD26 transfectants that CD26 presence enhances p38 phosphorylation, we established Karpas-299-CD26-siRNA as described in Materials and Methods. Whereas parental Karpas-299 cells have high level of CD26 surface expression, as shown previously (35), Karpas-299-CD26-siRNA cells exhibit low level of CD26 and a concomitant decrease in DPPIV enzyme activity (Fig. 4*A* and *B*). Importantly, Karpas-299-CD26-siRNA transfectants display decreased p38 phosphorylation level compared with parental Karpas-299 and missense Karpas-299-CD26-siRNA (Karpas-299-mis-CD26-siRNA) transfectants with unaltered CD26/DPPIV levels (Fig. 4*C*). Together, our findings show a clear association between CD26/DPPIV expression and increased p38 phosphorylation.